Hydrogeochemical signatures and human impact

A comprehensive analysis of groundwater quality on the semi-arid island of Curaçao

Wit, Mike R.J.; van Egmond, Jessie Lynn; Kruijssen, Titus P.; Bense, Victor F.; van Breukelen, Boris M.

DOI
10.1016/j.ejrh.2025.102555

Publication date
2025

Document Version
Final published version

Published in
Journal of Hydrology: Regional Studies

Journal of Hydrology: Regional Studies 60 (2025) 102555

Contents lists available at ScienceDirect

Journal of Hydrology: Regional Studies

journal homepage: www.elsevier.com/locate/ejrh

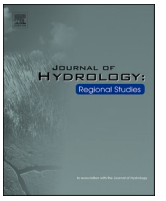

Hydrogeochemical signatures and human impact: A comprehensive analysis of groundwater quality on the semi-arid island of Curaçao

Mike R.J. Wit [a,*], Jessie-Lynn van Egmond [a], Titus P. Kruijssen [b], Victor F. Bense [b], Boris M. van Breukelen [a]

[a] Delft University of Technology, Faculty of Civil Engineering and Geosciences, Department of Water Management, Delft 2600, the Netherlands
[b] Wageningen University and Research, Hydrology and Environmental Hydraulics Group, Wageningen 6708, the Netherlands

ARTICLE INFO

Keywords:
Hydrochemistry
Groundwater pollution
SIDS
Urban wastewater
Source apportionment
Nitrate stable isotopes
Reverse osmosis

ABSTRACT

Study region: Island of Curaçao, Caribbean Sea
Study focus: Groundwater is a critical resource for many Caribbean islands. This study assessed the groundwater quality (main and trace elements, *E. coli*) of Curaçao during 4 subsequent wet seasons (2020–2024).
New hydrological insights for the region: Three main hydrochemical processes were identified with Principal Component Analysis (PCA): 1) seawater influence (median EC = 1900 µS/cm), 2) nutrient contamination, and 3) silicate weathering from altered basalts.
Elevated median nitrate concentrations (all 206 samples = 35 mg/L) are highest in urban areas (102 mg/L) suggesting wastewater leakage from cesspits. Lower Cl/B mass ratios (550) in urban areas compared to natural vegetated (1000) areas, indicate a wastewater source derived from reverse osmosis drinking water relatively high in Boron. Enrichment of $\delta^{15}N\text{-}NO_3$ and $\delta^{18}O\text{-}NO_3$ versus wastewater signatures indicates considerable occurrence of denitrification. Phosphate concentrations remain low (~0.1 mg/L), except for sites irrigated with large volumes of treated wastewater (>1 mg/L). Cl-B endmember mixing model showed 36 % wastewater contribution to groundwater, making it an important additional freshwater source given the semi-arid conditions. The findings underscore the value of comprehensive groundwater monitoring and the need for sanitation improvements. Addressing these challenges will benefit water management practices on Curaçao and similar islands. Additionally, it will improve groundwater quality, and groundwater-affected ecosystems, such as nearshore coral reefs.

1. Introduction

Groundwater is a critical resource for many small Caribbean islands, where freshwater availability is often constrained by low rainfall, high evaporation rates, and the absence of natural surface water. These Small Island Developing States (SIDS) therefore face urgent water resource challenges, further amplified by their small size, limited natural resources, and vulnerability to natural disasters

* Corresponding author.
E-mail addresses: m.r.j.wit@tudelft.nl (M.R.J. Wit), j.vanegmond@tewaii.com (J.-L. van Egmond), titus.kruijssen@wur.nl (T.P. Kruijssen), victor.bense@wur.nl (V.F. Bense), b.m.vanbreukelen@tudelft.nl (B.M. van Breukelen).

https://doi.org/10.1016/j.ejrh.2025.102555
Received 10 March 2025; Received in revised form 20 June 2025; Accepted 21 June 2025
Available online 27 June 2025

(Falkland, 1991). Groundwater supports domestic, agricultural, and industrial needs. However, population growth and increasing tourism in these often tourism-based economies (Cannonier and Burke, 2019), exert pressure on these already fragile groundwater systems.

Water availability and quality are pressing concerns for SIDS (Ahmed and Mishra, 2020). Fresh groundwater resources are often limited on these islands for several reasons. First, their large coastline to surface area ratio results in coastal groundwater experiencing salinization when abstraction rates are too high. Sea level rise further diminishes existing freshwater resources (Gohar et al., 2019). The lack of groundwater protection legislation in most SIDS (Holding et al., 2016) increases the risks of over-abstraction and salinization. Furthermore, climate change is projected to reduce groundwater recharge by up to 58 % in some SIDS by 2060, especially in the Caribbean and South Pacific, mainly attributed to altered precipitation and actual evapotranspiration (Holding et al., 2016). Urbanisation further increases water demand while likely diminishing groundwater recharge due to decreasing infiltration capacity.

Groundwater quality on islands is also significantly impacted by anthropogenic activities. Agricultural practices contribute to nutrient and pesticide pollution (Crabit et al., 2016; Gourcy et al., 2009; Rawlins et al., 1998), while inadequate wastewater disposal results in biological (i.e. pathogens) and nutrient groundwater contamination (Dillon, 1999; Falkland, 1999), as observed in the islands Barbados (Edwards et al., 2019), Bermuda (Jones et al., 2011), and Jamaica (Mandal and Haiduk, 2010). Additionally, high population densities further stress groundwater resources (Falkland, 1999), yet research on medium to smaller-sized islands remains limited.

Deteriorating groundwater quality affects both its use for human consumption and groundwater-receiving ecosystems of small islands. In recent decades, submarine groundwater discharge (SGD) has received increasing attention as an important pathway for land-based contaminants to the sea (Bejannin et al., 2020; Gordon-Smith and Greenaway, 2019; Santos et al., 2021). SGD significantly contributes to the nearshore nutrient balance (Santos et al., 2021) with potential negative outcomes for marine ecosystems (Houk et al., 2022). Excessive nutrient input leads to algal blooms that smother vulnerable coral ecosystems (D'Angelo and Widenmann, 2014; Zaneveld et al., 2016).

Anthropogenic pressures aside, groundwater vulnerability is also influenced by recharge rates. The hydrologic aridity index defined by Falkenmark and Chapman (1989) uses the ratio of annual precipitation to potential evaporation (P/E_p). Islands with $P/E_p < 0.75$ and $E_p > 1000$ mm are considered "dry, warm, and hot", making their groundwater systems particularly vulnerable due to relatively little recharge and less dilution of contaminants that enter the groundwater.

Caribbean islands vary widely in size, population density, socio-economic situation, and climate, so that the analysis of one particular island's groundwater challenges is unlikely to be representative for the entire region. However, the semi-arid island of Curaçao (444 km^2) is close to the median of 30 largest Caribbean islands (410 km^2) and presents unique circumstances for evaluating groundwater quality under challenging anthropogenic and natural conditions. Unlike other Caribbean islands of similar size, Curaçao has a relatively high population density (340 people per km^2) and a low P/E_p (0.24), making its groundwater system highly susceptible to depletion and pollution. These factors, along with potential impacts on the marine environment (Govers et al., 2014), make Curaçao a valuable case study for groundwater-related challenges in the region.

Previous hydrogeological studies on Curaçao's were conducted several decades ago and primarily focussed on salinity and its application for irrigation, identifying only the basaltic aquifers as a suitable source (Abtmaier, 1978). Louws et al. (1997) later observed considerable nitrate contamination near urban areas possibly related to leaking cesspits. In addition, they observed both groundwater freshening (45 %) and salinization (30 %) when compared to an earlier survey conducted in 1977 (Abtmaier, 1978). Freshening was thought to be linked to potable water or sewage leakage, although the results were inconclusive. A comparative study of the islands Aruba, Bonaire, and Curaçao by van Sambeek et al. (2000) identified dominant hydrogeochemical processes including calcite dissolution of the limestones, cation exchange, silicate weathering, and potassium fixation. More recently, an extensive study on the historical development of Curaçao's groundwater system by Kruijssen et al. (2024) showed that anthropogenic activities have substantially affected both groundwater levels and salinity. However, these studies did not demonstrate the direct link between sewage leakage, nutrient contamination, and the extent of groundwater pollution, as well as the fate of these pollutants.

This study aims to provide a comprehensive assessment of the groundwater chemistry and quality of Curaçao with a focus on quantifying sewage leakage impacts from urban areas on groundwater quality. Given the absence of a monitoring network, samples were collected from both private and public wells across varying depths. Analyses included major constituents, nutrients (NO_3, NH_4, PO_4, DOC), nitrate isotopes ($\delta^{15}N$, $\delta^{18}O$), trace elements, and microbial contamination (*E. coli*). Spatial groundwater quality patterns were examined, and multivariate statistical analysis reduced data dimensionality to identify relevant hydrogeochemical processes. Anthropogenic contamination was assessed through nutrient levels and wastewater tracers (Cl/Br, Cl/B), while nitrate isotopes were used to evaluate nitrate fate inside the aquifer. This study improves knowledge of groundwater quality in semi-arid island settings that lack official groundwater monitoring networks and provides insights for improved water management. In addition, it evaluates the effects of hydrogeochemical processes on seaward nutrient pollution, that in turn possibly improves groundwater-affected ecosystems, such as nearshore coral reefs.

2. Field site description

2.1. Geography and climate

Curaçao is one of the Leeward Islands and situated in the southern Caribbean Sea, 65 km off the coast of Venezuela (Fig. 2). It has a population of ~150,000, mostly concentrated in Willemstad surrounding Schottegat Bay (CBSC, 2011). Tourism significantly impacts the island, with annual visitors averaging 913,000 (2015–2021) and peaking at 1108,000 (441,000 stayover tourists) before the pandemic (CBSC, 2024b). The semi-arid tropical climate has an annual average temperature of 28 °C, with 580 mm of rainfall

primarily occurring as intense downpours during the wet season (Oct-Dec, Fig. 1).

2.2. Geological setting

2.2.1. Altered basalts

The Late Cretaceous Curaçao Lava Formation (CLF) (Kerr et al., 1996) comprises basalts, often observed as pillow lavas, covering ~54 % of Curaçao's interior surface (**Fig.** A. 1) (Klaver, 1987). The basalts are strongly weathered and fractured, and thus referred to as altered basalts (Beets, 1972), though this weathered zone strongly varies in thickness between 6 and 38 m (Abtmaier, 1978; Klaver, 1987). As such, they serve as the island's primary aquifer (Abtmaier, 1978; Kruijssen et al., 2024). These mafic, igneous rocks are rich in silica, magnesium, and iron (**Table** A. 1), and contain the silicate minerals albite ($2Na(AlSi_3)O_8$), anorthite ($Ca(Al_2Si_2)O_8$), (clino) pyroxene ($(Mg_{0.7}CaAl_{0.3})(AlSi_3)O_6$), and chlorite-like minerals ($(MgFeAl)_6\ (SiAl)_4O_{10}(OH)_8$) (Beets, 1972), including olivine ($(Mg, Fe)_2SiO_4$) (Kerr et al., 1996).

2.2.2. Sedimentary formations

The sedimentary formations consist of the Knip Group (KG, 10.6 % coverage) and Midden- Curaçao Formation (MCF, 8.1 % coverage). The KG lies unconformably over the CLF basalts, mainly exposed in the northwest and thinning out towards the middle of the island. It consists of silica-rich rocks (cherts), cherty limestones, pebbly mudstones, and clastic sediments (Beets, 1972). The conformably overlying MCF is composed of clastic sedimentary rocks, mainly exposed in central-Curaçao (Beets, 1977). Where the KG is absent, the MCF lies directly onto the basalts. The MCF contains mudstones, shales, sandstones, and fine-grained conglomerates (Molengraaff, 1929), reflecting turbidite sequences of submarine fan depositions (Beets, 1972). Limited permeability renders these sedimentary formations as less suitable aquifers.

2.2.3. Limestones

Limestones fringe the island and cover 24.7 % of the surface, subdivided into the Neogene Seroe Domi Formation (SDF) and Neogene-Quaternary limestone terraces (Vader Piet Formation, TNO-GDN (2021). The SDF consists of marine limestone, sometimes partially or completely dolomitized (Fouke et al., 1996) and covers the highest elevations along the leeward coast (Herweijer et al., 1977). In contrast, the limestone terraces occur at lower elevations along the coastline, making them vulnerable to salinization and generally less suitable aquifers due to the high permeability and proximity to the coastline.

2.2.4. Soils

Surface weathering has formed the characteristic brown-red soils, consisting mostly of sandy loam to silty-clayey loam soils with clay content averaging 10 % (de Vries, 2000). Kaolinite, montmorillonite, and illite minerals dominate the clay fraction. Furthermore, high heavy-metal contents of Cr, Ni, Zn, and Cu are also characteristic of Curaçao soils (de Vries, 2000).

2.3. Land use

Land use is derived from Steward et al. (2025) and comprises 77 % vegetation (shrubland (36 %), tree cover (26 %), grassland (13 %)), 19 % built-up areas, and 3 % is classified as bare soil. Only a small portion (<1 %) is identified as agricultural land, although small-scale agricultural activities might be overlooked. Most built-up areas concentrate around Schottegat bay with Willemstad and oil refinery complex. Approximately 17 % consist of urban areas (12 % dense urban and 5 % sparse urban areas). A large part of eastern Curaçao (~10 %: "Eastpoint") is privately-owned and inaccessible (Fig. 2).

The most significant land use changes over recent decades include reforestation in the west, driven by the establishment of nature conservation areas and the restriction of livestock grazing (Debrot, 2015), and continued urbanisation around Willemstad in the east, following rapid population growth (from 34,000 in 1920 to 150,000 in 1970). Over the past 50 years, the total population of Curaçao has remained relatively stable, although decreasing average household sizes and the substantial increase in tourism (stayover tourists:

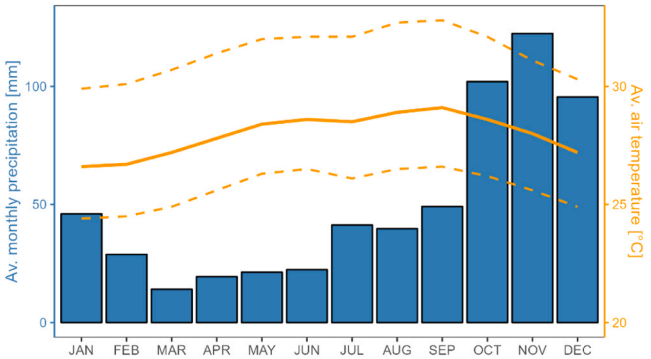

Fig. 1. Average monthly precipitation and air temperature for Curaçao (MDC, 2024).

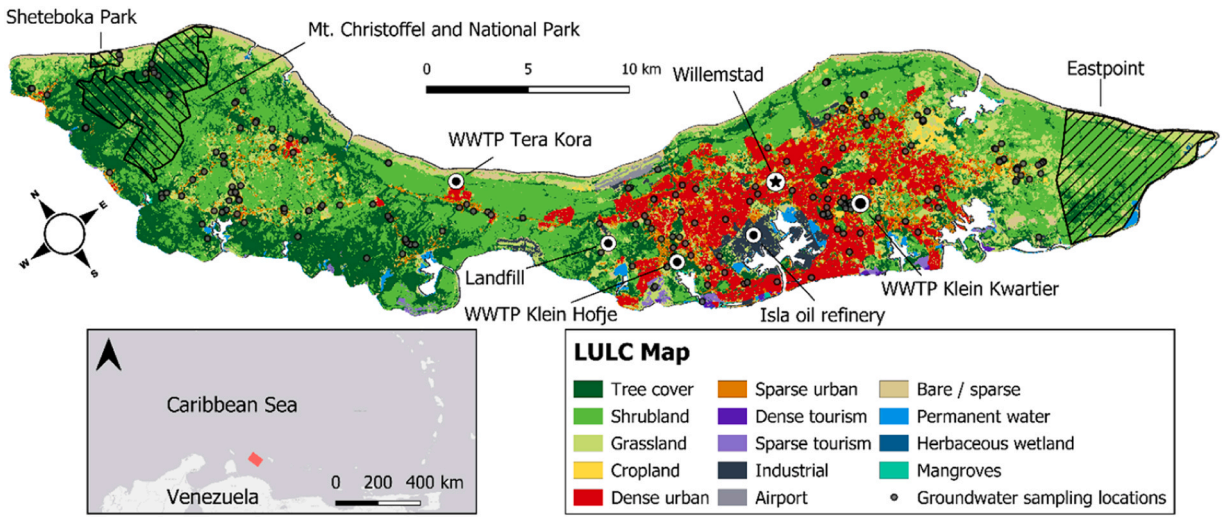

Fig. 2. Land use land cover (LULC) map of Curaçao after Steward et al. (2025) with groundwater sampling locations and points of interest.

100,000 in 1970 to 500,000 in 2023) (CBSC, 2024a) has exerted additional pressure on urbanisation rates.

2.4. Water management

2.4.1. Hydrology

Curaçao lacks perennial surface water, except for natural springs and artificial lakes behind dams that fill up during the wet season. The island's catchments are drained by ephemeral streams, locally referred to as '*rooien*', that flow during extensive rainfall and mostly drain into the several inland bays (STINAPA, 1977). Grontmij and Sogreah (1968) estimated groundwater recharge to be approximately 2–4 % of annual rainfall (average ~17 mm). Although this estimate is based on limited data and is now considered outdated, it remains the only recharge estimate available for the island/region and comparable recharge rates (0.1–5 %) have been reported for other (semi-)arid regions (Scanlon et al., 2006). Due to high potable water prices private wells are commonly used for irrigation, filling of swimming pools, and car washing. The number of residential wells is estimated at 7835 (CBSC, 2021), which has tripled over the last 30 years (CIWC, 2020). Moreover, well drilling is not regulated leading to unchecked groundwater abstraction, illustrated by year-round abstraction in agricultural areas for irrigation.

2.4.2. Drinking water

Drinking water is produced by two desalinization plants with a combined capacity of 50,000 m^3/d in 2017 (UNOPS, 2018). From 2016–2020, annual production was roughly 80 % of the total capacity (~14.7 million m^3/yr, CBSC 2021). The first plant, established in 1911, initially only became a backup for the water supply from groundwater (Van Meeteren, 1945). From 1962 onwards, only desalinated drinking water was used (Kruijssen et al., 2024). At first this process was based on evaporation using a thermal distillation process, although the Santa Barbara plant, operational since 2005, exclusively uses reverse osmosis (RO) technology (Bonnélye et al., 2007). By 2014, production was split between 70 % RO and 30 % evaporators (Kim-Hak et al., 2014), but recent upgrades made the transition to exclusively RO.

According to a 2013 study by Vitens Evides International (VEI) non-revenue losses across the water distribution network amounted to 24–28 %, equally split between physical losses (leaks) and apparent losses (inaccurate meters, illegal connections) (VEI, 2013). Assuming similar leakage rates in 2016–2020, physical losses (12–14 %) totalled 1.76–2.05 million m^3 annually. Applying this leakage to Willemstad's surface area (~117 km^2) yields 16 mm of additional recharge, similar to recharge from rainfall. However, localised recharge near pipelines is likely several orders of magnitude higher. Depending on how these water pipes are placed, either buried or above ground, a fraction might be susceptible to evaporation, making this leakage flux uncertain. In any case, desalinated water possibly has a significant contribution to groundwater availability and quality through drinking water leakage, wastewater seepage after use, and irrigation with treated wastewater.

2.4.3. Wastewater management

Wastewater management on Curaçao is limited, with only 19 % of the population connected to centralized sewage systems (CBSC, 2011). The majority relies on cesspits (77 %) or septic tanks (3 %), resulting in untreated wastewater seeping into the groundwater. Terminology for these systems is often used inconsistently (Strande et al., 2023), and the absence of standardized designs for Curaçao further complicates understanding leakage pathways and related water quality. Van der Molen and Buth (1993) mention cesspits and soak pits as common disposal methods on Curaçao to infiltrate wastewater directly into the subsurface. However, regions with low permeability or high groundwater levels are unsuitable for these systems. Densely populated areas on fractured basalts are particularly

vulnerable to contamination due to rapid wastewater infiltration and short residence times.

A cesspit is typically a holding tank that collects and stores sewage, though often designed to allow effluent percolation into the subsurface (Adegoke and Stenstrom 2019, see **Fig.** B. 1). While cesspits require periodic sludge removal via vacuum trucks (DOW, 1991), a lack of regulated inspection on cesspit emptying or placement often results in suboptimal functioning. As a result, domestic wastewater seeps into the groundwater largely untreated. Although this leakage poses serious risks of groundwater contamination, it also significantly enhances groundwater recharge, especially in the densely populated areas. Previous estimates by Louws et al. (1997) suggest cesspit infiltration in Willemstad contributes approximately 1 million m^3 of wastewater annually, comparable to natural recharge rates (DOW, 1991). However, these estimates are outdated due to changes in population and might have been too conservative. Considering current household drinking water sales (~7.5 million m^3/yr, Aqualectra 2021), 50–80 % drinking water to wastewater conversion rate, and 81 % of population using onsite disposal systems; up to 3.0 – 4.7 million m^3 cesspit leakage might be more realistic.

Collected sewage is largely treated at the two wastewater treatment plants (WWTP) of Klein Hofje (62 %) and Klein Kwartier (34 %), see Fig. 2 for their locations. Both facilities frequently exceed capacity, leading to partial treatment of direct discharge into terrestrial or marine environments (UNOPS, 2018). However, both WWTPs play an important role in supplying valuable fresh water. Klein Hofje distributes ~490,000 m^3/yr of treated effluent for irrigation of nearby golf courses and horticultural businesses (UOOW, pers. comm.). Klein Kwartier uses infiltration ponds for treated wastewater with downstream wells abstracting ~70,000 m^3/yr of groundwater for agricultural and hotel use (UOOW, pers. comm.). While the plant's total capacity is 640,000 m^3/yr, the volume directed to the infiltration ponds remains uncertain. Nevertheless, effluent discharge from both WWTPs likely contributes to substantial localized groundwater recharge.

3. Methods

3.1. Field sampling

3.1.1. Groundwater sampling locations

Groundwater samples were collected to represent the island's geological and land use variation during four subsequent wet season field campaigns (October-January, 2020–2023), in line with previous studies also conducted during the wet season (Abtmaier, 1978; Louws et al., 1997). The wet season was chosen due to its influence on hydrogeological dynamics, including increased recharge. A total of 273 samples were obtained from 206 locations (Fig. 2), including both public and private deep wells, hand-dug wells, and springs. Accessibility challenges limited sampling in certain areas such as privately-owned Eastpoint (Fig. 2) and regions with fewer wells. Fig. 3 shows the distribution of groundwater samples across geological formations, highlighting overrepresentation of the basaltic CLF because of abundant wells in Willemstad, and underrepresentation in limestone areas due to limited wells.

3.1.2. Sampling procedure

Samples were collected from open hand-dug wells (36.4 %) and (semi-) closed deeper boreholes (63.6 %). The hand-dug wells are typically several meters wide, while most boreholes are 0.23 m in diameter. All sampled wells were only cased at the top to prevent collapse and thus collect groundwater across their entire depth profile. Consequently, samples are considered integrated mixtures of water from all intercepted aquifer layers, although the exact contribution of each layer is unknown. In a subset of wells, electrical conductivity (EC) depth profiles were measured to explore vertical heterogeneity. These revealed variations with depth in some cases, underscoring the importance of sampling depth, although these data are not further presented here. Sample collection methods depended on well characteristics, such as presence of pre-installed pump or windmill, access to the well, and groundwater depth (Fig. 4).

Where possible, stagnant water was removed prior to sampling to ensure representative groundwater quality. Generally, the

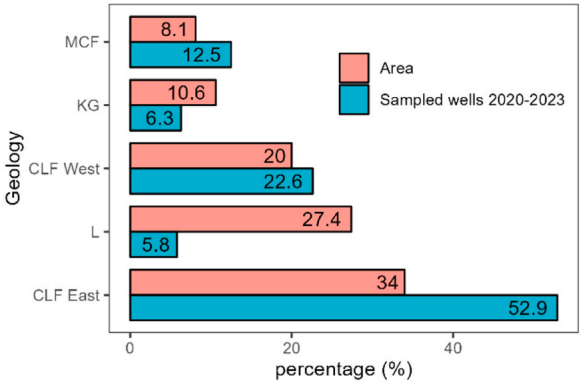

Fig. 3. Percentage of groundwater wells sampled per geology ordered by the respective surface area. CLF = Curaçao Lava Formation, MCF = Midden-Curaçao Formation, KG = Knip Group, and L = Limestone.

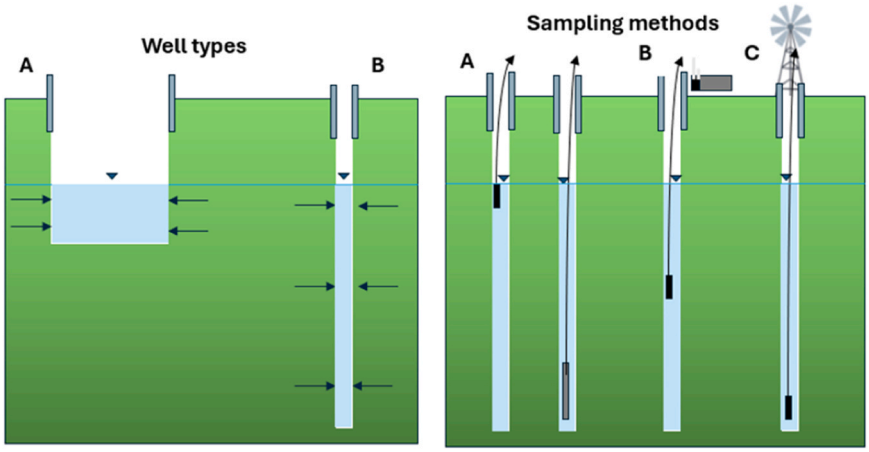

Fig. 4. Left: well types on Curaçao with uncased wide hand-dug wells (A) and uncased deep boreholes (B). Right: groundwater sampling methods with A) grab samples using a bottle/bucket from the top of the groundwater or using a stainless-steel bailer from the bottom of the well, B) using a peristaltic sampling pump approximately between the middle and the bottom of the well, and C) using a pre-installed pump from the bottom of the well.

sampling steps were as follows:

- **Pre-installed pump:** If a pre-installed pump was present this was used to collect the sample. If frequently used (daily/weekly), no flushing was needed. Otherwise, the pump operated for 10 min to purge the well and retrieve ambient groundwater. Hydrochemical parameters (electrical conductivity (EC), pH, dissolved oxygen (DO), oxidation-reduction potential (ORP), and temperature) were measured until readings stabilized before sampling.
- **Peristaltic pump:** If groundwater levels were < 9 m below the surface and no pump was present, a peristaltic sampling pump was used (Solinst, model 410). Samples were collected several meters below the water table after hydrochemical parameters stabilized, serving as a proxy for purging.
- **Bailer:** If groundwater levels were > 9 m below the surface and no pre-installed pump was present, samples were collected without purging the well with a stainless-steel bailer (Solinst, model 429 2") from the bottom of the well.
- **Bottle:** Samples from 2021 were all collected from the top groundwater using a bottle on a rope without purging the well, unless pre-installed pumps were available.

Additionally, other sample types were collected to identify water or sources of contamination. Rainwater ($n = 23$) was collected for a varying number of collection days and rainfall amount, wastewater samples ($n = 12$) were collected from the influent and effluent of the WWTPs, and seawater ($n = 5$) along the coast.

Hydrochemical parameters (EC, pH, DO, ORP, and Temp) were measured directly in the field using a pre-calibrated multi-meter (Ponsel Odeon, 1413 µS/cm, pH 4 & 7, and ORP 240 mV). A flow-through cell was used for pumped samples or a separate container for grab samples. Stabilized readings were recorded before collection. Four 15 mL filtered samples (0.20 µm Chromafil PTFE membrane) were collected for ion chromatography (IC), inductively coupled plasma mass spectrometry (ICP-MS), and dissolved organic carbon (DOC) analysis, with one reserved as back-up. Two additional unfiltered 50 mL samples were collected for alkalinity titration within 24 h. During the 2022–2023 fieldwork, an additional filtered 50 mL was collected for stable nitrate isotope analysis. Vials were rinsed with filtered sample water and filled without headspace, except for ICP-MS/DOC samples, which required subsequent acidification.

Alkalinity was determined within 24 h using a sulfuric acid titration kit (Hach) with bromecresol green/methyl red indicator powder. Results were expressed as mg/L $CaCO_3$ and converted to HCO_3 concentrations (100 mg/L $CaCO_3 = 122$ mg/L HCO_3). Samples were stored cold and dark during fieldwork and transferred to the Carmabi lab on Curaçao on the same day. Cation and trace element samples (ICP-MS) were acidified with HNO_3 (69 %) and DOC samples with HCl (38 %) to pH < 2. Samples were refrigerated at < 4°C both before and after shipping to the Netherlands, where they were analysed (see Section 3.2). Furthermore, microbial contamination (*E. coli*) was assessed qualitatively using 3 M Petrifilm *E. coli* plates, applying 1 mL of sample and incubating the plates in duplicate for 24–36 h at roughly 28 °C (unairconditioned average room temperature for lack of an incubator). Results were expressed as Colony Forming Units (CFU) per 100 mL of sample.

3.2. Chemical analysis

Anions (F, Cl, NO_2, Br, NO_3, SO_4) were analysed using IC (Methrohm 818) and main and trace elements (Na, K, Ca, Mg, Si, B, Fe, Mn, V, Zn) using ICP-MS (Analytik Jena PlasmaQuant). NH_4 and PO_4 concentrations were analysed using a colorimetric method (Seal Analytical Discrete Analyzer, AQ400). These measurements were all performed in the Waterlab of the TU Delft. DOC was measured using a Shimadzu TOC Analyzer at the University of Amsterdam.

Stable nitrogen ($\delta^{15}N$) and oxygen ($\delta^{18}O$) isotopes of nitrate were analysed at the Stable Isotope Facility, British Geological Survey, UK. Samples were prepared in duplicate for analysis, by converting dissolved nitrate to nitrous oxide (N_2O) via the titanium reduction method of Altabet et al. (2019). International nitrate standards (USGS34, USGS35, IAEA-NO3 and IAEA NICO6) were prepared at a concentration of 1 mg/l NO_3-N and converted to N_2O following the same Ti reduction procedure as the samples. The $\delta^{15}N$ and $\delta^{18}O$ of produced N_2O gas was analysed using an Elementar iso FLOW GHG, coupled to a visION isotope ratio mass spectrometer. Isotope standard materials are reported on international scales, $\delta^{15}N$ relative to atmospheric N_2 (AIR) and $\delta^{18}O$ on Vienna Standard Mean Ocean Water (VSMOW) in permil (‰) following:

$$\delta(‰) = \frac{R_{sample} - R_{standard}}{R_{standard}} \times 1000 \quad (1)$$

where R is the isotopic ratio of $^{15}N/^{14}N$ and $^{18}O/^{16}O$ in the sample and standard. Standards were chosen to bracket a wide isotope range (34.9 ‰ for $\delta^{15}N$ and 85.4 ‰ for $\delta^{18}O$) and the average long term (multiyear) repeatability of these standards is < 0.7 ‰ for $\delta^{15}N$ and < 0.8 for $\delta^{18}O$.

3.2.1. Data validation

Analytical quality was verified using the charge balance (%) for major ions (Appelo and Postma, 2005). Errors in the charge balance were evenly distributed between negative and positive values. For 77 % of the samples the error was < 5 %, for 19 % between 5 – 10 %, and for 4 % the error was > 10 %. These results were generally considered acceptable (Appelo and Postma, 2005). Samples with > 10 % charge imbalance were omitted from statistical analysis.

3.3. Hydrochemical calculations

Spatial information such as geology, land use, and population data were assigned to each sampling location. Ionic delta concentrations (ΔC) were calculated to identify deviations from seawater mixing, aiding in the detection of relevant hydrogeochemical processes (Appelo and Postma, 2005; Fidelibus et al., 1993):

$$f_s = \frac{Cl_{sample} - Cl_{rain}}{Cl_{sea} - Cl_{rain}} \quad (2)$$

$$C_{TMix} = (1 - f_s) \bullet C_f + f_s \bullet C_s \quad (3)$$

$$\Delta C = C_{OBS} - C_{TMix} \quad (4)$$

Where f_s is the seawater fraction in the mixed sample calculated using the Cl concentration in the sample, rainwater, and seawater, C_f and C_s are the freshwater and seawater concentrations for a given ion, C_{TMIX} and C_{OBS} are the expected concentration from conservative seawater mixing and the observed concentration, and ΔC is the ionic delta concentration for a given sample.

Additionally, several ion combinations were used as tracers, such as Cl/Br (Alcalá and Custodio, 2008; Davis et al., 1998; McArthur et al., 2012) and Cl/B mass ratios (Kloppmann et al., 2008a, 2008b) to detect urban wastewater leakage, and SO_4/Cl for identifying additional SO_4 sources related to oxidation or reduction processes with organic material. Next, a simple 3-endmember linear mixing model with Cl and B was used to estimate the wastewater contribution to the groundwater by solving the mass balance Eqs. 5–7 (Muir and Coplen, 1981; Vázquez-Suñé et al., 2010). As endmembers, median concentrations of collected rainwater, wastewater, and seawater were used (**Appendix** E, **Table** E. 2).

$$f_{groundwater} = 1 = f_{rain} + f_{wastewater} + f_{sea} \quad (5)$$

$$Cl_{groundwater} = Cl_{rain}f_{rain} + Cl_{wastewater}f_{wastewater} + Cl_{sea}f_{sea} \quad (6)$$

$$B_{groundwater} = B_{rain}f_{rain} + B_{wastewater}f_{wastewater} + B_{sea}f_{sea} \quad (7)$$

with f the proportion of the different endmembers to the groundwater and Cl and B their respective concentrations. Furthermore, mineral saturation indices (SI) were calculated using the geochemical modelling code PHREEQC v3.73 (Parkhurst and Appelo, 2013) with the WATEQ4F database.

3.4. Multivariate statistics

Multivariate statistics are widely used in environmental studies with large complex datasets to organize and extract useful information. These methods are common tools in hydrochemical studies where many parameters are measured per sample (Cloutier et al., 2008; Güler et al., 2012; Monjerezi et al., 2012) and can provide a quantitative description of environmental measurements, describe the inter-relationship of environmental drivers, and detect contamination sources (Dupont et al., 2020). In this study, principal component analysis (PCA) was applied as an exploratory analysis to assess chemical variations in groundwater samples. PCA reduces data dimensionality by correlating hydrochemical parameters and extracting new uncorrelated variables, or principal components (Güler et al., 2012). These components were then used to identify underlying geochemical and anthropogenic processes influencing groundwater quality. Components with eigenvalues > 1 were selected for further interpretation.

Data preparation

Preparing the hydrochemical dataset for multivariate analysis involved several steps. First, for wells with multiple samples, average concentrations for all parameters were calculated. Parameters with > 50 % of values below the detection limit (<DL) or having > 50 % missing data were excluded. This process retained 19 parameters for analysis: pH, DO, Na, K, Ca, Mg, Cl, HCO_3, SO_4, NO_3, PO_4, NH_4, Si, Fe, Mn, B, Br, V, and Zn. For concentrations <DL, the DL value was substituted (Cloutier et al., 2008), and missing values (2 samples for Fe, V, and Zn) were replaced with the parameter median. As most parameter distributions were positively skewed, log-transformations were applied to approximate normal distributions (Monjerezi et al., 2012), except for pH and DO which showed low skewness (respectively 0.6 and 0.3, see **Table** C. 1). To ensure equally weighted variables, the log-transformed data was standardized to unit variance by subtracting the mean and dividing by the standard deviation to achieve mean = 0, sd = 1.

4. Results and discussion

4.1. General groundwater composition

Groundwater in Curaçao shows a large variability in EC, ranging between 113 and 58,000 μS/cm with mean and median values of 3515 and 1894 μS/cm, while Cl concentrations are respectively 969 and 341 mg/L. Elevated nutrient levels occur within the groundwater for NO_3 (median = 35.2 ± 88.1 mg/L), while PO_4 levels are generally low (median = 0.1 ± 2.9 mg/L). In addition, the groundwater is characterised by high median concentrations of HCO_3 (443 ± 197 mg/L), Si (26.8 ± 13.5 mg/L), B (420 ± 495 μg/L), and V (111 ± 108 μg/L).

Groundwater temperatures are relatively stable, with a mean and median of 29.7 °C, exceeding the 10-year average air temperature (28.1°C, Meteorological Department Curaçao). The pH fluctuates between 6.2 and 8.5, with a mean and median of 7.2, indicating slightly basic conditions. Dissolved oxygen (DO) varies from 0 to 9.2 mg/L with a mean and median concentration of 3.4 and 3.2 mg/L (respectively 43 % and 41 % saturation). Similar DO levels in open wells and boreholes suggest that some level of oxygen is present in the groundwater, likely due to the weathered and fractured characteristics of the island's dominant basaltic aquifer. This is further supported by the mean and median ORP values of 109 and 125 mV, indicating moderate oxidative conditions. Groundwater quality assessments show its general suitability for irrigation purposes. Table 1 summarises key hydrochemical parameters for different applications, while comprehensive descriptive statistics are provided in Table C. 1.

4.2. Principal component analysis

4.2.1. PC1 – Fresh-saline interaction

Principal component analysis identified four components explaining 64.5 % of the total variance (Table D. 1). Most of the variance is contained in PC1 (30.8 %), which is strongly associated with Cl, Na, Ca, Mg, K, and SO_4 (loadings between 0.67 and 0.94). This component reflects oceanic influence with increasing salinity and related ions, encompassing processes such as increasing salinity towards the coast, remnants of past sea transgressions, and the presence of paleo seawater in certain geological formations (e.g. Mid. Curaçao Formation and Knip Group sedimentary aquifers). Additionally, shallow fresh groundwater mixing with deeper, more saline groundwater in certain wells may contribute to this variability.

4.2.2. PC2 – Nutrient contamination

PC2 explains 15.5 % of the variance and is dominated by PO_4, NH_4, ORP, SO_4, and NO_3. Negative loadings for PO_4 (-0.74) and NH_4 (-0.69) contrast with positive loadings for ORP (0.64), SO_4 (0.51), and NO_3 (0.49). This component likely reflects nutrient contamination by sewage leakage into the groundwater. Interestingly, the inverse correlation between PO_4 and NH_4 versus NO_3, ORP, and SO_4 seems to reflect the distance from a contamination source. Near contamination sources PO_4 and NH_4 are highest, while redox potential

Table 1
Water quality standards for drinking water, irrigation water of typical crops grown on Curaçao, and for livestock. Values between brackets show percentage of measured groundwater wells above the relevant threshold.

Parameter	Drinking water (WHO[a])	Irrigation (FAO[b])				Livestock (FAO)[b]
		Corn	Tomato	Squash/ zucchini	Coconut	
Cl mg/L	250 / 150[c]	525	875	1575	-	250
	(66 % / 84 %)	(33 %)	(21 %)	(14 %)		(66 %)
EC μS/cm	1500	1700	2500	4900	-	5000*
	(71 %)	(57 %)	(34 %)	(20 %)		(20 %)
NO_3 mg/L	50	-	-	-	-	110
	(39 %)					(18 %)
E. coli* *	0	-	-	-	-	0
CFU/100 mL	(78 %)					(78 %)

* < 1500 μS/cm is considered 'excellent' and < 5000 μS/cm 'very satisfactory'
** Only measured in 120 wells in 2021–2023
[a] WHO, 2009
[b] (FAO, 1994)
[c] Dutch drinking water standard

and oxidant levels (NO_3 and SO_4) are lower. Down the flow path, PO_4 precipitates or adsorbs onto mineral surfaces, while NH_4 oxidizes to NO_3 following Eq. 8. Mixing with increasingly oxic water is indicated by higher ORP and SO_4 levels. Furthermore, reducing conditions may generate elevated NH_4 and PO_4 concentrations and might indicate natural sources within the aquifer.

Nitrification reaction (Wilhelm et al., 1994):

$$NH_4^+ + 2\ O_2 \rightarrow NO_3^- + 2H^+ + H_2O \quad (8)$$

4.2.3. PC3 – Water-rock interaction

PC3 accounts for 10.6 % of the variance and is associated with HCO_3 (0.73), Si (0.62), and V (0.59), reflecting silicate weathering. Basaltic rock weathering produces dissolved silica, cations, and bicarbonate, while consuming acid and increasing the pH (Appelo and Postma, 2005), illustrated in Eq. 9. In addition, weathering releases trace elements such as vanadium, commonly enriched in basaltic aquifers due to volcanic rock composition (Bellomo et al., 2014).

General basalt weathering to kaolinite (Tweed et al., 2005):

$$Ca_{0.58}Na_{0.42}Al_{1.58}Si_{2.42}O_{8\ (s)} + 1.58H_2CO_3 + 2.47H_2O \rightarrow 0.79\ Al_2Si_2O_5(OH)_{4\ (s)} + 0.58\ Ca^{2+} + 0.42Na^+ + 1.58\ HCO_3^- + 0.84H_4SiO_4 \quad (9)$$

4.2.4. PC4 – pH and DO

The final component correlates with pH (0.79) and DO (0.71), potentially indicating organic matter oxidation. This process consumes oxygen, reducing DO levels and lowering pH. The three major processes identified by PC1-PC3 - groundwater salinity, nutrient contamination, and water-rock interaction - will be further addressed in **Sections 4.3–4.5**.

4.3. Groundwater salinity

4.3.1. Chloride concentrations

Based on Cl concentration, the collected groundwater is generally considered fresh (<250 mg/L, 34 %) or brackish (250–1000 mg/L, 47 %), while 17 % is brackish-saline (1000–5000 mg/L) and 2 % is saline (>5000 mg/L), as illustrated in Fig. 5. Despite the brackish conditions, most groundwater remains suitable for irrigation (Table 1). The lowest chloride concentrations are found in the basaltic aquifer in the island's interior, with lower median Cl levels in the eastern basalts (263 mg/L) compared to the western basalts (379 mg/L). This might be explained by additional freshwater recharge from urban sewage leakage. Salinity increases towards the coast, but higher salinities are also observed in the sedimentary aquifers (Knip Group and Mid. Curaçao Formation). These elevated levels likely indicate fossil seawater associated with their submarine depositional original and lower permeability with limited aquifer flushing (Abtmaier, 1978). Additionally, higher salinity is found near dyke intrusions in the northeast Ronde Klip area.

4.3.2. Background salinity

Proximity to the ocean generates significant wet and dry salt deposition on Curaçao. During rainfall, these salts are flushed to the groundwater, but high evaporation rates concentrate the salt levels of recharge. The average Cl concentration in collected rainwater (n = 23), for a varying number of collection days and rainfall amounts, is 18 mg/L (68 µS/cm). When considering 85 % evaporation, the Cl content of the remaining water, or wet deposition, will increase to 120 mg/L (~450 µS/cm).

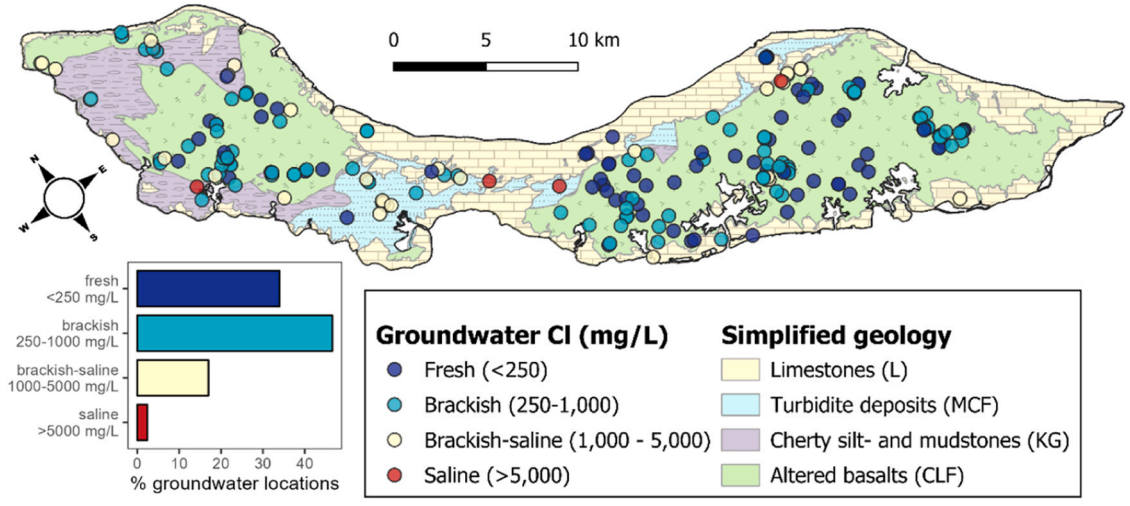

Fig. 5. Left: groundwater salinity class distribution. Right: spatial chloride concentrations for 2020–2023. Geology after Beets (1972).

However, dry deposition outside the wet season further increases salt input. Teixeira et al. (2023) determined the total Cl deposition on a small island in the Pacific and found average Cl deposition rates of 26 mg m^{-2} d^{-1} at 1500–2000 m from the coast. Assuming 15 % of annual rainfall (600 mm) remains after evaporation yields 90 mm/yr or 0.25 mm/d. Dry deposition then contributes roughly 104 mg/L Cl, bringing the total Cl input to ~224 mg/L. Although this estimate is likely an overestimation due to greater inland washout on Curaçao (up to 10 km), it aligns with the 30th percentile of groundwater Cl concentrations (229 mg/L). Therefore, this estimated Cl level can be considered a natural "baseline" salinity from sea spray and high evaporation. This baseline salinity approaches the WHO drinking water standard (250 mg/L) and highlights the island's inherent vulnerability to saline conditions.

Additional processes also influence groundwater salinity. Factors that increase salinity include irrigation return flow with enhanced evaporation, water-rock interactions, seawater intrusion and past transgressions, enhanced interception of salt aerosols by vegetation, and evaporation from dam reservoirs. Conversely, processes such as enhanced infiltration, and leakage of wastewater and drinking water pipelines lowers salinity levels below the baseline.

4.3.3. *Hydrochemical facies*

Fig. 6 shows the major ion composition of groundwater samples. The most dominant hydrochemical facies is Ca-Mg-Cl (48 %), followed by Ca-Mg-HCO_3 (25 %, mostly fresh groundwater), Na-Cl (23 %), and Na-HCO_3 (3 %, indicating freshening). The abundance of Cl-water types (64 %) reflects island conditions with marine influence, consistent with the interpretation above. Surprisingly, Mg-water types dominate over Ca, possibly indicating the importance of Mg-rich silica weathering and/or dolomite dissolution being more relevant than calcite dissolution (see Section 4.4). Two distinct Mg-SO_4 water types are observed near cemeteries.

Most groundwater types indicate potential salinization or saline conditions (Ca-Mg-Cl and Na-Cl), although it is difficult to distinguish between historical and ongoing salinization based on these data. This assumes, however, that only base exchange processes affect proportions of cations in groundwater. When processes such as significant silicate weathering become dominant, interpreting hydrochemical facies becomes challenging and may lead to the misidentification of salinization. In addition, the large inputs of Cl from sea spray might already partly explain these 2 hydrochemical facies.

Given Curaçao's semi-arid climate, widespread unregulated groundwater abstraction, and irrigation practices, active salinization by seawater intrusion likely occurs in some areas (Abtmaier, 1978; Kruijssen et al., 2024; Louws et al., 1997). Since the altered basalt aquifers retain most fresh water, signalling salinity shifts in these areas is particularly important. Fig. 7 shows the spatial pattern of hydrochemical facies indicating potential salinity changes. Agricultural regions in the southeast show signs of groundwater salinization by reverse cation-exchange (Ca-Mg-Cl) caused by irrigation-return flow. Typically, abstracted groundwater is subjected to evaporation that increases salt concentrations of infiltrating water, while high abstraction rates also risk attracting deeper saline water. During return flow, the displacement of Ca^{2+} and Mg^{2+} on the exchange-sites for Na^{+} leaves Ca-Mg-Cl water types. Some areas also reveal freshening signals, though no distinct spatial pattern emerges. To confirm salinity trends, a long-term groundwater quality analysis using historical data is needed, but this falls outside the scope of this study.

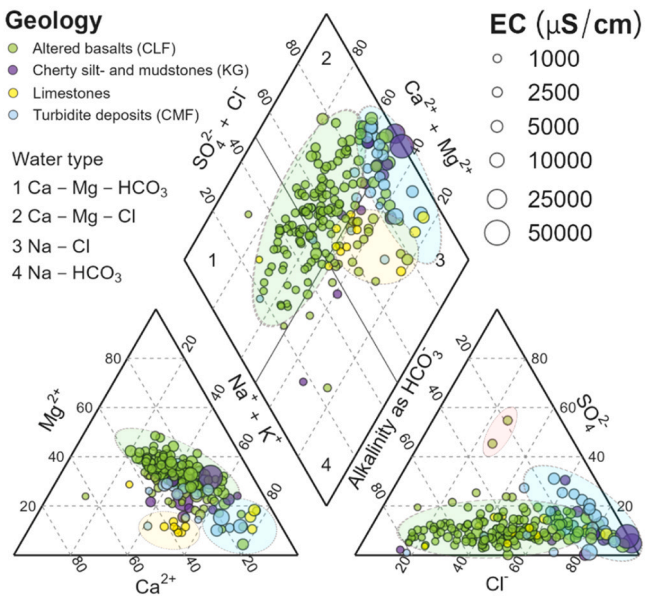

Fig. 6. Piper diagram showing relative major ion concentrations in groundwater samples (2020–2023), categorised by geological formation with hand drawn highlight areas: large transition of HCO_3 to Cl water types for basalts (green), Cl dominated water types in sedimentary aquifers (blue), Ca water types on limestones (yellow), and SO_4 water types (red). Generally, more Na-Cl water types with related higher EC are observed in the sedimentary Knip Group and Curaçao Midden Formation, while Ca-Mg-Cl and Ca-Mg-HCO_3 water types dominate in the Curaçao Lava Formation.

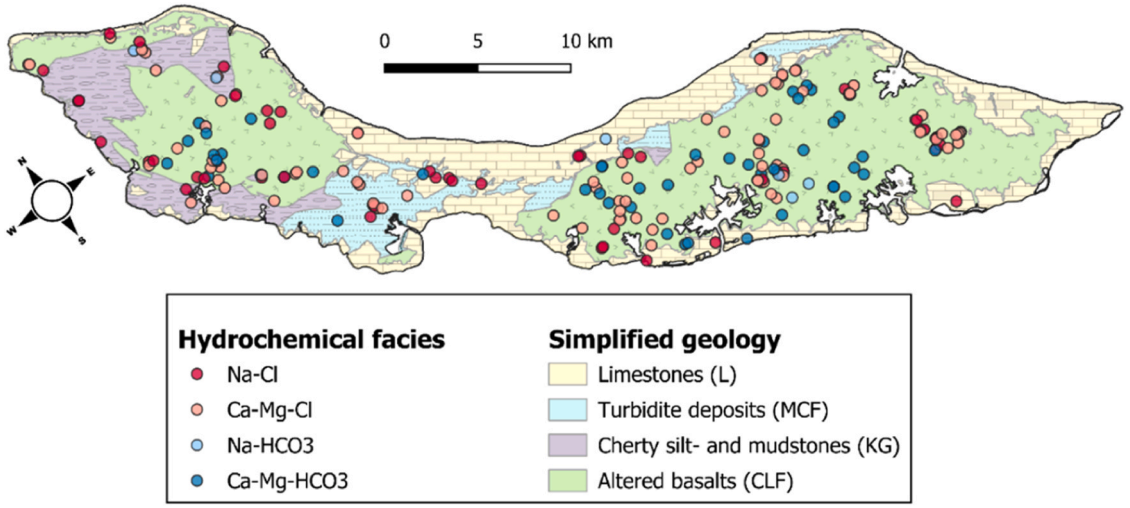

Fig. 7. Groundwater hydrochemical facies distribution showing areas of potential freshening ($Na\text{-}HCO_3$) or salinization (Ca-Mg-Cl). Geology after Beets (1972).

4.4. Water-rock interaction

4.4.1. Mineral equilibria

Elevated partial pressures of CO_2 in Curaçao's groundwater (median $\log pCO_2 = -1.52 = 3.02\ 10^{-2}$ atm) compared to atmospheric

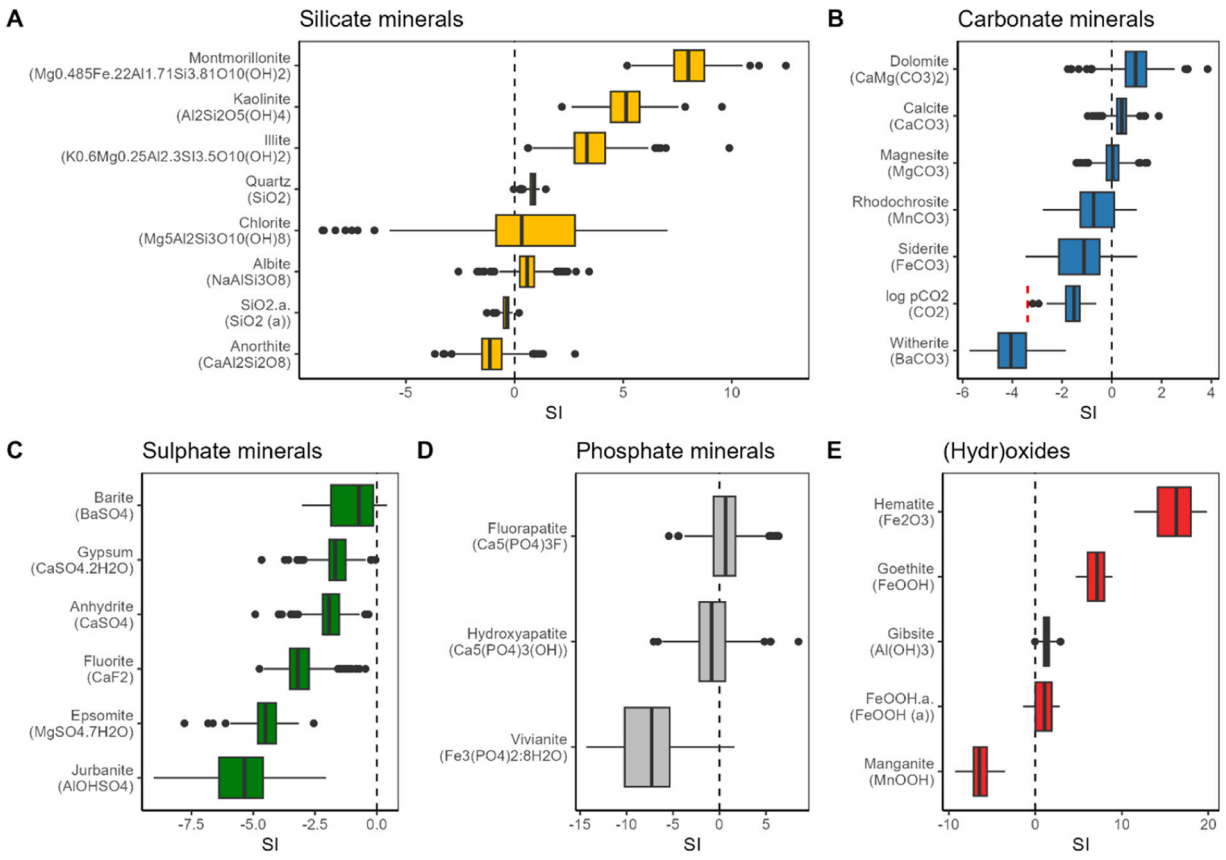

Fig. 8. Mineral saturation indices for groundwater samples. Red dashed line B) indicates atmospheric pCO_2. Values < 0 indicate undersaturation and values > 0 super-saturation.

levels (log $pCO_2 = -3.38 = 4.17\ 10^{-4}$ atm) indicate enhanced mineral weathering, partially driven by organic matter degradation from sewage inputs (Eiswirth and Hötzl, 1997). PHREEQC calculations show dissolved CO_2 ranging from 0.21 – 8.6 mmol/L (median = 0.92 mmol/L), facilitating basalt weathering which releases dissolved silica and cations, while consuming acid and increasing pH (Appelo and Postma, 2005), as shown in Eq. 9. Fluoride (median = 0.1 mg/L) and vanadium (median = 111 µg/L), often associated with volcanic rock weathering (Bellomo et al., 2014; Podgorski and Berg, 2022), were generally below drinking water guideline values (1.5 mg/L for F (WHO)). Although no international standard exists for vanadium, a limit of 140 µg/L has been adopted in Italy (Russo et al., 2014) and approximately 40 % of groundwater samples exceed this threshold. Mineral equilibrium calculations (Fig. 8A) reveal that primary silicate weathering (SI anorthite < 0 + partly albite) leads to the formation of clay minerals (kaolinite, montmorillonite) and hematite (Fe_2O_3, Fig. 8E) on Curaçao (de Vries, 2000), products typical of basalt weathering (Beckman et al., 1974).

When enough Ca and Mg are supplied, secondary carbonate minerals such as dolomite (91 %), calcite (89 %), and magnesite (53 %) become super-saturated, suggesting precipitation potential (Fig. 8B). Of the sulphate minerals (Fig. 8C) only some locations were super-saturated with respect to barite (16 %), while gypsum and anhydrite remain under-saturated. Phosphate mineral saturation (Fig. 8D) for fluorapatite (61 %) and hydroxyapatite (32 %) points to sewage-derived PO_4 inputs and subsequent precipitation with Ca.

4.4.2. *Mixing and reaction processes*

To capture subtle changes in groundwater chemistry during freshening/salinization processes, deviations from the seawater mixing line (ionic deltas) were calculated for each groundwater location (Fig. 9). Fig. 9A shows ΔNa is enriched up to 10 % seawater content indicating cation-exchange and freshening possibly linked to sewage leakage. Between 1 % and 10 % seawater mixing, both positive and negative ΔNa values suggest freshening and salinizing conditions at different locations. Above 10 % seawater mixing, Na is consistently depleted as it is being replaced by Ca and Mg, which show enrichment (Fig. 9B-C). This process explains the prevalence of Ca-Mg-Cl hydrochemical facies in the groundwater.

Additionally, Ca and Mg may be derived from carbonate and Mg-rich silicate weathering. Unlike Na, ΔK is almost exclusively depleted, likely due to the sorption of K^+ onto illite clays (Bruggenwert and Kamphorst, 1979; Griffioen, 2001; Sawhney, 1972) as a common weathering product of basalt. Fig. 9E shows that HCO_3 is consistently above the seawater mixing line, driven by mineral weathering and DOC oxidation from sewage input. Interestingly, the ΔHCO_3 concentrations range from 4 to 14 meq/L, likely constrained by calcite and dolomite precipitation (SI > 0) induced by elevated Ca and Mg concentrations.

The elevated Mg compared to Ca concentrations further supports Mg-rich silicate weathering (e.g. chlorite SI < 0 for 50 % of samples) as a dominant process rather than carbonate dissolution (SI > 0 for calcite + dolomite). After adjusting for seawater influence (ΔMg) and cation-exchange, a significant correlation between silica and Mg was identified for the basaltic aquifer (Fig. F. 2). The found relationship of ΔMg = -0.102 + 2.18 Si reflects weathering of silicate, following the stoichiometry of olivine:

$$\underset{2}{Mg_2SiO_4} + 4H_2CO_3 \rightarrow \underset{2}{2Mg^{2+}} + \underset{4}{4HCO_3^-} + \underset{1}{H_4SiO_4} \quad (10)$$

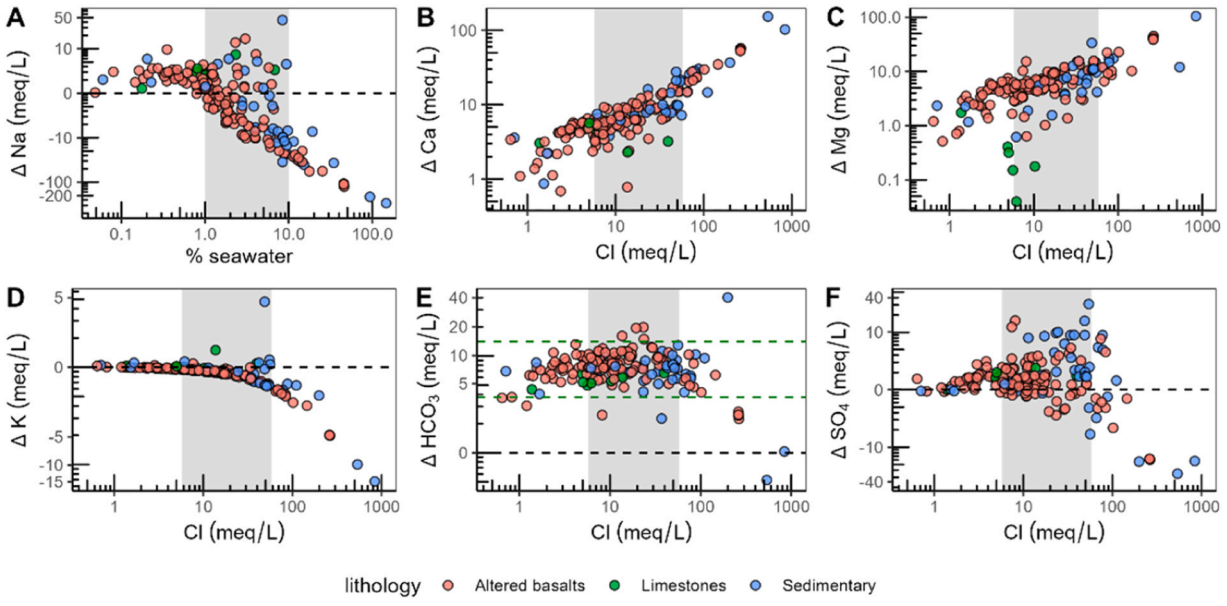

Fig. 9. Ionic delta concentrations for main ions plotted against Cl or seawater percentage. Negative values indicate ion depletion with respect to the freshwater-seawater mixing line; positive values indicate enrichment. The shaded area represents 1–10 % seawater mixing zone. Sedimentary aquifers include the Knip Group and Mid. Curaçao Formation.

In contrast, Ca appears decoupled from silica, indicating complex precipitation-dissolution dynamics, potentially linked to sewage-derived PO_4 and HCO_3 released from silicate weathering.

4.4.3. Sulphate sources

Sulphate concentrations in groundwater exceed values expected from the seawater mixing line, as shown by positive ΔSO_4 (Fig. 9F). Fig. 10 alternatively shows SO_4 consumption (-) and production (+) based on the Cl/SO_4 ratio scaled to the seawater ratio (0.14). Most groundwater samples show SO_4 production, particularly in the sedimentary turbidite aquifer of the Mid. Curaçao Formation, likely attributed to dissolution of marine evaporites. Some of these locations fall on the gypsum dissolution line (Fig. F. 1), suggesting gypsum dissolution as a source of SO_4.

Furthermore, higher SO_4 production is observed for the eastern basaltic aquifer near Willemstad, compared to the western, more naturally vegetated basaltic aquifer. Elevated SO_4 in Willemstad is likely attributed to anthropogenic sources such as atmospheric deposition of SO_2 from traffic and oil refinery emissions and sewage leakage (Torres-Martinez et al., 2020). Additionally, two sites near cemeteries showed high SO_4 concentrations, with corresponding Mg-SO_4 as hydrochemical facies, possibly reflecting localized anthropogenic inputs.

4.5. Groundwater nutrient contamination

4.5.1. Nitrogen

Nitrogen primarily occurs as nitrate (NO_3) in groundwater. The median NO_3 concentration across all samples is 35 mg/L, with elevated levels observed in urban areas (median 102 mg/L) and cropland regions (64 mg/L) (Fig. 11). Inside urban areas, higher concentrations are associated with denser populations, suggesting sewage leakage from cesspits as a major source. Some extremely high NO_3 levels, reaching up to 792 mg/L, are found in the western part of the island linked to agricultural activities and livestock farming.

Nitrite (NO_2) concentrations exceeding 0.5 mg/L were detected in 11 % of wells, suggesting active (de)nitrification processes. In addition, 7 % of wells contained NH_4 concentrations > 1 mg/L, with values up to 205 mg/L. Elevated NH_4 concentrations are mostly restricted to the sedimentary aquifers of the Mid. Curaçao Formation, potentially indicating contributions from seawater origin or reducing conditions with a natural origin. NH_4 from sewage is likely nitrified to NO_3 in the subsurface, as indicated by sufficient DO levels (average 3.4 mg/L or 43.1 %, oxic conditions).

An anomaly in the high NO_3 concentrations within Willemstad shows lower concentrations downstream of WWTP Klein Kwartier, where treated wastewater is infiltrated using infiltration ponds (Section 2.4.3). The large infiltration rate of artificial recharge, with low nutrient levels due to treatment, biological uptake, and subsurface passage, seems to displace the polluted groundwater observed in other parts of the city up to several kilometres downstream (Fig. 12).

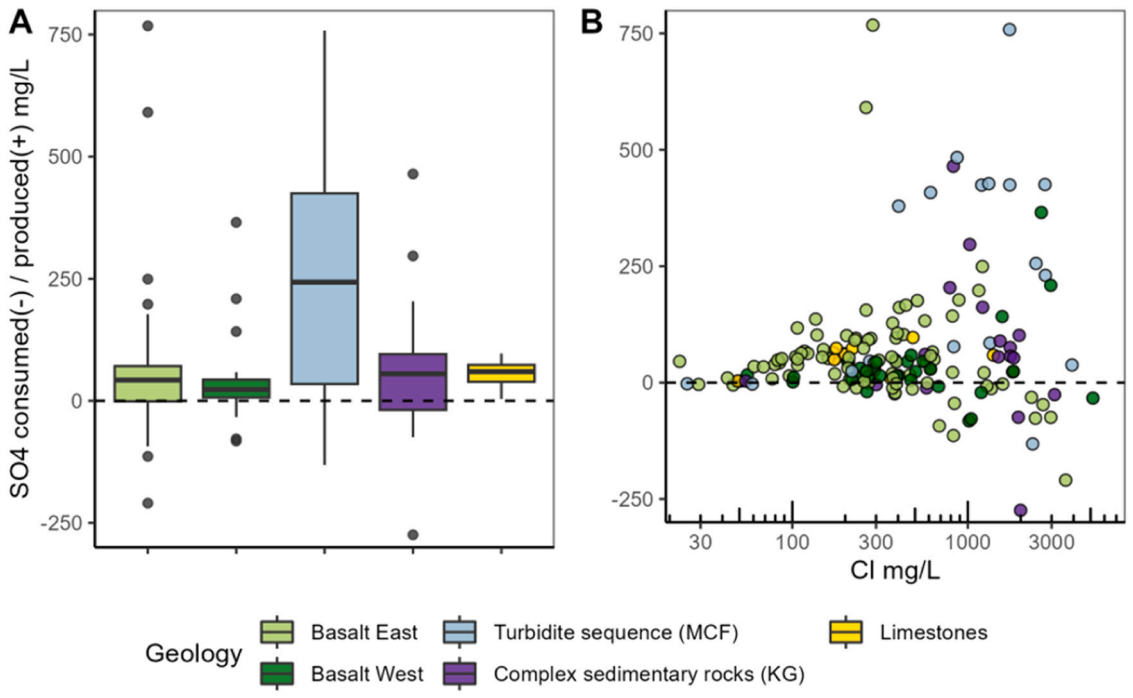

Fig. 10. SO_4/Cl ratio scaled to seawater (0.14), illustrating SO_4 consumption (-) and production (+) across geological formations. Five outliers omitted by zooming in.

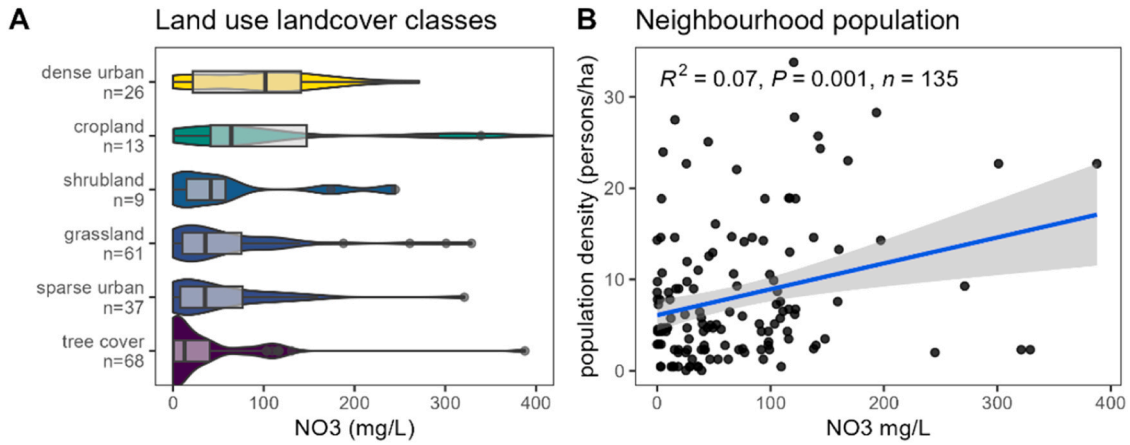

Fig. 11. Groundwater nitrate concentrations A) for different LULC classes (Steward et al., 2025) and B) plotted against neighbourhood population density (CBSC, 2011). The (significant) low p-value with low R^2 indicates a significant correlation, though explaining little of the variability. One outlier of 790 mg/L is omitted for cropland, 1 sample for bare/sparse LULC class and NO_3 < dl is omitted.

4.5.2. Nitrate isotopes

Stable nitrate isotopes ($\delta^{15}N$ and $\delta^{18}O$) were used to determine NO_3 sources and fate inside the aquifer. Groundwater NO_3 isotopic values ranged between + 8.9 to + 30.3 ‰ for $\delta^{15}N$ and + 6.1 to + 20.8 ‰ for $\delta^{18}O$ (n = 31). Comparable values were observed in *rooi* discharge (ephemeral streams) of + 18.7 to + 28.4 and + 11.9 to + 16.4 ‰ for $\delta^{15}N$ and $\delta^{18}O$, respectively (n = 4). Two untreated and treated wastewater samples exhibited $\delta^{15}N$ values of + 8.8 and + 10.4 and $\delta^{18}O$ values of + 4.2 and + 7.3, respectively. Fig. 13 shows the nitrate isotope data together with ranges of potential NO_3 sources. Sewage and manure waste are enriched in heavier ^{15}N relative to other sources of NO_3, but are indistinguishable based on NO_3 isotopes alone (Kendall, 1998). However, based on high NO_3 concentrations below urban areas a significant part of NO_3 is expected to derive from sewage leakage (Section 4.5.1).

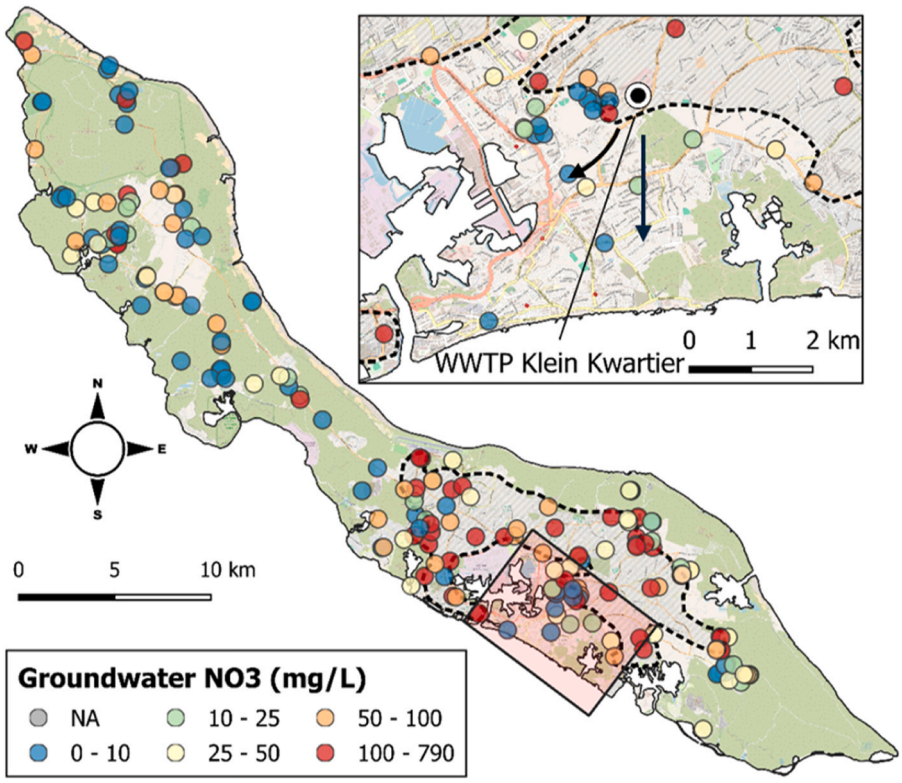

Fig. 12. Groundwater nitrate concentrations for 2020–2023. Dashed area indicates urban area of Willemstad with higher NO_3 levels. In-zoom map shows urban area with lower NO_3 anomaly due to displacement with artificially recharged treated wastewater from WWTP Klein Kwartier.

During storage, treatment or leakage of sewage and manure, volatilization of ammonia (NH_3) causes a large enrichment of $\delta^{15}N$ in the residual NH_4. Subsequent nitrification results in enriched NO_3 in the range of + 5 to + 25 ‰ (Xu et al., 2016; Xue et al., 2009). Values of $\delta^{18}O$-NO_3 depend on local conditions due to the incorporation of ^{18}O from water and atmospheric oxygen. Source ranges were therefore determined using the approximated nitrification equation after Mayer et al. (2001):

$$\delta^{18}O_{NO3} = \quad 2/3 \quad \delta^{18}O_{H2O} + \quad 1/3 \quad \delta^{18}O_{O2} \tag{11}$$

Calculated $\delta^{18}O$-NO_3 values for sewage/manure sources ranged between + 5.4 and + 9.0 ‰, using $\delta^{18}O$-H_2O = -3.6 and + 1.7 ‰ (respectively the minimum and maximum values in the studied groundwater, see Table C. 1) and + 23.5 ‰ for atmospheric $\delta^{18}O$ (Kroopnick and Craig, 1972).

Fig. 13 shows that most samples are enriched compared to the sewage/manure isotopic composition indicating denitrification. This process preferentially converts the lighter ^{14}N and ^{16}O isotopes to N_2 and N_2O, resulting in heavy isotopes enrichment in the residual NO_3 (Kendall and Caldwell, 1998). Higher nitrate concentrations in collected samples associated with low $\delta^{15}N$ and $\delta^{18}O$, and vice versa, further emphasise denitrification. Linear regression of groundwater and *rooi* discharge samples yielded a slope of 0.54 ($\varepsilon N/\varepsilon O$ = 1.9, $R^2 = 0.76$), consistent with denitrification trends from other groundwater studies that report $\varepsilon N/\varepsilon O$ slopes ranging from 1.3 to 2.3 (Böttcher et al., 1990; Fukada et al., 2003; Harris et al., 2022; Otero et al., 2009). Granger and Wankel (2016) showed that ratios of $\delta^{15}N/\delta^{18}O > 1$ occurred when NO_2 formed by denitrification is re-oxidised to NO_3 by integrating lower $\delta^{18}O$ of groundwater.

Six groundwater locations have $\delta^{18}O$-NO_3 values that coincide with isotopic ranges typical of sewage or manure sources (Fig. 13), suggesting minimal denitrification. Among these, GW084 and GW088 (agricultural areas), and GW101 and GW103 (urban regions), likely reflect nitrate isotopic signatures close to their source. Additionally, two locations in limestone (GW075 and SP005), show similar isotopic patterns, potentially due to the high permeability and limited residence time in limestone, which limit denitrification. This is particularly relevant for the coastal region, where extensive limestone formations combined with built-up areas may cause sewage leakage with little attenuation before discharging into the marine environment.

Denitrification estimates

The extent of denitrification was estimated using Eq. 12 (Ostrom et al., 2002; Otero et al., 2009):

$$DEN(\%) = \left[1 - \quad e^{(\delta_{sample} - \quad \delta_{source})/\varepsilon}\right] \quad \times 100 \tag{12}$$

where δ_{sample} and δ_{source} are respectively the isotopic ratios in the sample and source (‰) and ε is the enrichment factor (‰). Using literature ε values from −4.0 ‰ to −15.9 ‰ (Böttcher et al., 1990; Fustec et al., 1991) and assuming an initial $\delta^{15}N$-NO_3 value of + 8.3 ‰ from measured untreated wastewater, denitrification ranged from 0.9 % to 99.5 % (median 88 %) using ε = -4 ‰, and 0.2–74.1 % (median 41 %) for ε = -15.9 ‰. These are estimates due to variations in local conditions that influence ε values and the degree of fractionation (Kendall, 1998; Ostrom et al., 2002).

Microbial denitrification requires DO levels below 2 mg/L (Cey et al., 1999; Gillham and Cherry, 1978) and the availability of DOC or other electron donors. Most groundwater on Curaçao, however, showed higher DO levels (73 % >2 mg/L), suggesting unfavourable denitrifying conditions. Still, a weak negative correlation between $\delta^{15}N$-NO_3 and DO, together with enriched nitrate isotopic data suggests denitrification occurs (result not shown). This is potentially due to anaerobic conditions at the micro-scale (Koba et al., 1997), but anaerobic conditions may also develop within the aquifer matrix, while fractures remain largely aerobic. Additionally, the mixing of groundwater from various depths in long wells can conceal oxygen gradients within the aquifer, potentially hiding the fact that deeper groundwater is anaerobic. Improved ε estimates would improve denitrification quantification, but current findings already indicate that denitrification accounts for tens of percentages reduction in NO_3 pollution in groundwater on Curaçao. In addition,

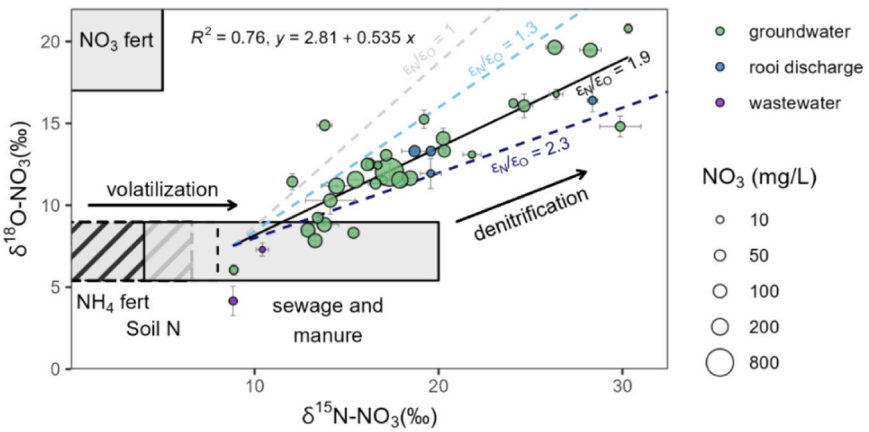

Fig. 13. Stable nitrate isotopes plotted together with nitrate concentrations in groundwater, rooi discharge, and wastewater. Grey boxes illustrate potential nitrate sources with $\delta^{15}N$ values from literature (Xue et al. (2009) and references therein), whereas local $\delta^{18}O$-NO_3 source values of soil N and sewage/manure were determined using nitrification Eq. 10. $\varepsilon_N/\varepsilon_O$ = 1.3 from Fukada et al. (2003) and $\varepsilon_N/\varepsilon_O$ = 2.3 after Böttcher et al. (1990).

nitrate isotopic enrichment in *rooi* discharge samples suggest a drained groundwater origin with previous subsurface passage, which is important when understanding nutrient sources from this pathway.

4.5.3. Phosphate and DOC

Elevated NO_3 concentrations in groundwater are strongly associated with sewage leakage, suggesting that other nutrient inputs (e.g. PO_4 and DOC) may originate from the same source. However, clear correlations (e.g. with densely populated areas) or distinct spatial patterns for PO_4 and DOC are less apparent. This is likely due to differences in their environmental behaviour and the presence of additional sources.

PO_4 concentrations in groundwater are generally low, with 21 % of wells showing levels < 0.03 mg/L. This is primarily due to sorption and precipitation processes, which retard PO_4 mobility. This is supported by equilibrium conditions for the phosphate mineral fluorapatite (see Fig. 8). The diffusive leakage from cesspits therefore does not appear to significantly elevate PO_4 concentrations. Instead, highest PO_4 concentrations (>1 mg/L) are observed under varying conditions, including in saline wells, near the landfill, and in areas with large-scale use of treated wastewater. For example, downstream of the WWTP Klein Kwartier infiltration pond, PO_4 varies between 1.2 and 5.6 mg/L. Similarly, golf courses southwest of WWTP Klein Hofje which utilize treated wastewater for irrigation show PO_4 concentrations of 1.4–12.2 mg/L in groundwater. These findings highlight that while localised cesspit leakage may allow for sufficient PO_4 sorption, the infiltration of larger volumes of treated wastewater results in more significant PO_4 breakthrough. This reflects lower removal of P compared to N during wastewater treatment on Curaçao, with implications for sites where this wastewater is discharged or reused.

DOC was measured in groundwater during the wet season 2021–2022, with concentrations ranging from 0.6 to 42 mg/L (median = 3.1 mg/L). Although a weak correlation exists between DOC and PO_4 ($p = 0.039$, R^2=0.04), a large variation was observed. Oxidation of DOC under oxic conditions likely reduces its persistence in groundwater compared to NO_3. This might explain why no clear spatial pattern exists. However, a notably high DOC concentration (36 mg/L) was measured near the landfill (Fig. 2), indicating a localised source.

4.5.4. Other wastewater tracers: E. coli, Cl/Br and Cl/B

Measurements of *E. coli* in groundwater serve as an indicator of faecal contamination and potential wastewater pollution. Between 2021 and 2023, *E.* coli was detected in 78 % of sampled wells, making this water unsuitable for consumption (median and mean = 275 and 2020 CFU/100 mL). While no significant correlation was found between *E. coli* and nutrient concentrations, inclusion in a principal component analysis revealed a weak correlation with PO_4 and NH_4 that might indicate sewage leakage. However, the exact origin of *E. coli* remains unclear, as it may originate from sewage leakage, livestock, and/or pets).

The Cl/Br ratio is commonly used in hydrochemical studies as a wastewater tracer (Alcalá and Custodio, 2008; McArthur et al., 2012). Both Cl and Br behave conservatively in the environment, but Br is strongly depleted in wastewater compared to other water types due to NaCl-loaded wastewater. This results in higher Cl/Br mass ratios (600−1400) in wastewater (Alcalá and Custodio, 2008; McArthur et al., 2012), compared to natural waters such as rain and seawater (approximately 280). This contrast can be used to identify contamination sources. However, environmental conditions such as arid coastal climates, volcanic rocks, and urban wastewater – factors relevant to Curaçao – can produce overlapping Cl/Br ratios (Alcalá and Custodio, 2008). This complicates source identification, making Cl/Br a less ideal tracer for these conditions.

The Cl/B ratio may provide a more distinct tracer for wastewater derived from reverse osmosis (RO) water. Drinking water is

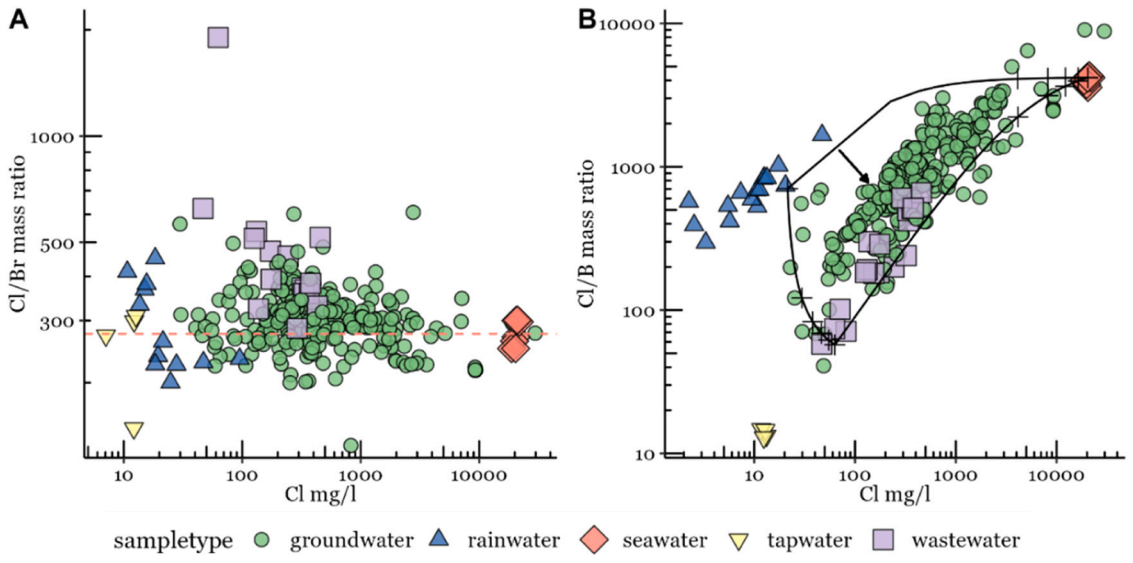

Fig. 14. A) Mass ratios of Cl/Br and B) Cl/B vs Cl with linear mixing lines where crosses depict 20 % mixing.

enriched in boron (B) due to its incomplete removal during the desalinization process with membranes (Kloppmann et al., 2008b). This enrichment is observed in a low Cl/B mass ratio (13) of desalinated drinking water on Curaçao, but also derived wastewater retains this signature. Additionally, the use of sodium perborate in detergents and bleaching agents further increases B levels in wastewater (Stueber and Criss, 2005; Waggott, 1969). Combined with boron's relatively conservative behaviour, high solubility, and low concentrations in most waters (Barth, 1998), this makes the Cl/B ratio a useful tracer for the identification of RO water and (RO-derived) wastewater inputs to groundwater. While Cl/B ratios have been used to trace geothermal waters (Dotsika et al., 2010) or treated wastewater (Kaehler and Kenneth, 2003; Kloppmann et al., 2008a), this study applied this ratio for the first time to track the infiltration of wastewater derived from RO drinking water in groundwater. This approach offers a valuable addition to existing methods (e.g. boron isotopes) in environments increasingly reliant on RO-based water supply systems.

Fig. 14 compares Cl/Br and Cl/B ratios to Cl concentrations for various water samples. Cl/Br ratios in Fig. 14A indicate that both rainwater and tap water follow the seawater mass ratio (275, molar ratio of 600), while wastewater samples indeed fall above this seawater ratio as expected. Groundwater shows significant variation with most samples falling along the rain-seawater mixing line or exceeding it, possibly suggesting wastewater influence. However, overlapping sources make Cl/Br ratios less conclusive in this context.

In contrast, Cl/B ratios provide a clearer indication of wastewater contributions to groundwater. Under natural conditions, groundwater is expected to follow the rain-seawater mixing line. Fig. 14B, however, shows most groundwater samples falling below this line, indicating contributions from a low Cl/B source, likely wastewater. This effect is most pronounced for lower Cl concentrations, indicating potential groundwater freshening due to wastewater leakage. Groundwater samples can be considered a mixture of three hydrochemical endmembers: rain, seawater, and wastewater (wastewater evolution from tap water is described in **Appendix** E). Linear endmember mixing model calculations using B and Cl concentrations indicate that groundwater comprises 61 % infiltrated rainwater, 37 % wastewater, and 2 % seawater (median contributions). While RO has only recently become the dominant technology in desalinization plants on the island (see Section 2.4.2), the associated increase in B concentrations in infiltration wastewater has therefore been relatively recent. As a result, older groundwater likely exhibits a weaker B signal compared to younger water that is more influenced by wastewater leakage. Estimates of the wastewater contribution to groundwater using Cl/B ratios likely represents a lower boundary. This confirms sewage leakage as a significant additional recharge source, particularly in urban areas.

Fig. 15B illustrates the lowest Cl/B ratios, associated with RO-derived sewage, occurring beneath urban areas, further confirming the impact of sewage. These findings demonstrate that the RO-specific Cl/B tracer is a valuable tool for identifying wastewater leakage, particularly in regions where Cl/Br ratios are inconclusive. With the increase in RO desalinization plants globally – 68 new facilities in the Caribbean alone since 2007 (Blach, 2015; CaribDA) – this approach could be useful for islands and coastal regions facing similar challenges. To our knowledge, this study is the first to apply Cl/B ratios to trace wastewater derived from desalinated RO drinking water in groundwater systems.

4.6. Environmental implications

The diffuse leakage of cesspits into groundwater on Curaçao has led to elevated nutrient concentrations. Particularly vulnerable are the densely urbanized, permeable coastal limestone areas, where sewage leakage undergoes minimal attenuation before reaching the ocean. Additionally, large fluxes of (partially) treated wastewater, either directly infiltrated into the subsurface or used for irrigation, have resulted in PO_4 breakthrough and lower N:P nutrient ratios in groundwater for these areas, which may become relevant upon discharge into the marine environment. The direct discharge of (untreated) wastewater further intensifies these concerns, not only contributing to eutrophication but also introducing pathogens and organic micropollutants that may threaten marine ecosystems and public health. Together, these challenges in wastewater management increase the risk of environmental degradation, potentially causing ecological damage to nearshore ecosystems such as coral reefs.

Islands facing similar challenges could benefit greatly from policies focused on (ground)water quality monitoring to identify pollution sources and signal changes over time. Wastewater management improvements should prioritise coastal areas particularly vulnerable to seepage, e.g. densely populated zones with permeable subsurface conditions (limestones) and shallow groundwater levels, where natural attenuation in the unsaturated zone is limited.

4.7. Heterogeneity and sampling bias

4.7.1. Heterogeneity

Significant spatial variation in groundwater composition on Curaçao has long been recognized, with relatively fresh wells often located near saline ones (Henriquez, 1962). This study also observed substantial differences in groundwater quality over short distances, particularly in salinity and nutrient contamination. These variations reflect the island's complex geology, characterized by fractured and weathered aquifers (Abtmaier, 1978; Beets, 1972; Kruijssen et al., 2024) that act as conduits for rapid solute transport. This geological complexity, combined with localized pollution sources from cesspits, small-scale agriculture, decomposing animals in wells, but also groundwater abstractions, results in the sometimes-heterogeneous patterns in groundwater quality.

The location of wells relative to the local groundwater flow direction and their relative position to pollution sources further influences "observed" water quality. Well depth is another critical factor contributing to heterogeneity. Deeper wells may intercept saline groundwater that significantly alters the quality compared to shallow wells. Additionally, fully penetrating wells may yield mixed groundwater samples across depth intervals, depending on pumping practices and aquifer characteristics. These factors underscore the complexity of interpreting groundwater quality data in heterogeneous aquifer systems.

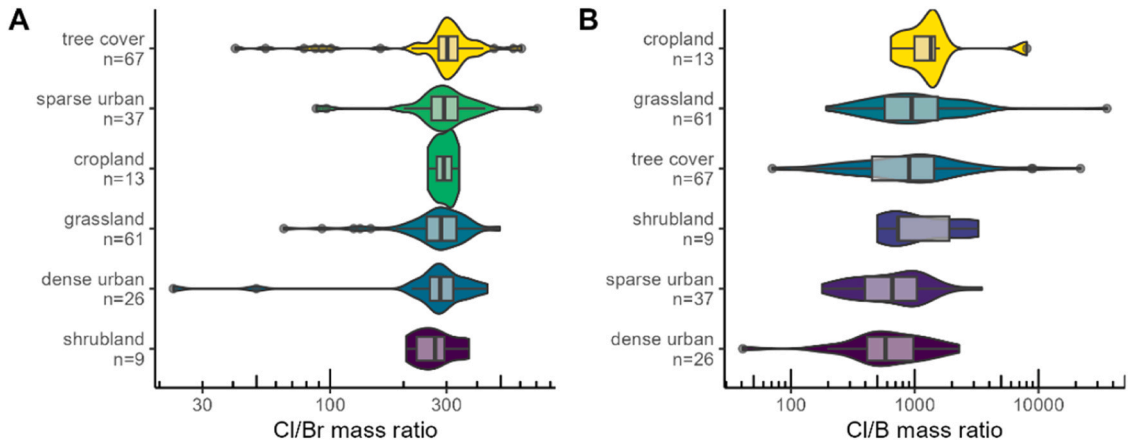

Fig. 15. A) Cl/Br and B) Cl/B mass ratios for different LULC classes with violin and boxplots to illustrate sample distribution. Lowest Cl/B ratios observed for urban areas related to RO water enriched with B.

4.7.2. Sampling bias and monitoring

Most groundwater wells in Curaçao are located near households, especially in densely populated areas with higher nutrient concentrations. This introduces a sampling bias towards anthropogenically influenced groundwater, likely overestimating average/median nutrient concentrations. Similar findings were reported by McArthur et al. (2012), who observed that domestic wells were often impacted by leaking cesspits. Martinez-Santos et al. (2017) also noted that many rural domestic wells were influenced by on-site sanitation systems. This bias highlights the importance of designing and maintaining a groundwater monitoring network that accounts for variations in land use, pollution sources, and well depths. Monitoring at multiple depths on several locations would provide useful insights into the vertical extent of groundwater contamination and interaction between shallow and deeper aquifers. In addition, samples in this study were collected during the wet season, when dilution may lower groundwater concentrations. Groundwater quality during the dry season is likely to show higher concentrations due to reduced recharge and dilution. Future monitoring should therefore include the dry season to capture seasonal fluctuations and improve understanding of temporal groundwater quality variability.

While this sampling bias may be less representative of the broader groundwater quality, it does reflect the water quality to which people are directly exposed. As such, domestic wells remain valuable for assessing public health risks, despite their biased distribution. Future monitoring efforts would benefit from including domestic wells within a systematically designed network to capture both human exposure and the overall status of the aquifer system.

5. Conclusion

This study characterised the groundwater quality and assessed the impact of sewage leakage on the semi-arid island of Curaçao through multiple sampling campaigns. Principal component analysis (PCA) identified saline-freshwater mixing, nutrient contamination, and silicate weathering as the dominant processes affecting groundwater quality. Most groundwater in Curaçao is brackish (median 1900 μS/cm) due to sea spray and mixing with groundwater of marine origin. Naturally high Cl background concentrations (median 224 mg/L) determined from wet and dry deposition highlights the island's inherent vulnerability to saline conditions. Silicate weathering in the main basaltic aquifers contributes to elevated Si, Mg, and trace metal concentrations (e.g. vanadium). Cation-exchange is indicated by negative ΔNa, where Na is being replaced by Ca, and results in the dominant Ca-Mg-Cl water type (48 %).

Cesspit leakage in densely populated areas was linked to elevated nitrate concentrations in groundwater (median 102 mg/L). Low Cl/B mass ratios (550) further confirmed sewage contamination derived from reverse osmosis (RO) drinking water. This appears to be first study to apply Cl/B ratios for tracing sewage derived from RO drinking water and validates Cl/B as a suitable tracer for wastewater in similar environments, particularly given the increase in RO desalination plants worldwide. An endmember mixing model using Cl and B estimated a wastewater contribution of 36 % to the groundwater, indicating significant additional anthropogenic recharge.

Enriched stable nitrate isotope ratios revealed active denitrification in groundwater with conversions up to tens of percentages. The presence of dissolved oxygen above 2 mg/L suggests either localised denitrification under anaerobic micro-scale conditions or the presence of more oxic conditions prevailing within fractured zones, with anoxic conditions elsewhere in the aquifer. However, coastal limestone areas with built-up areas may cause sewage leakage with little attenuation before discharging into the marine environment, posing risks to nearshore ecosystems.

Unlike nitrate, phosphate concentrations remain low (~0.1 mg/L) due to precipitation (e.g. fluorapatite) and adsorption during transport. However, sites irrigated with large volumes of treated wastewater from wastewater treatment plants exhibited elevated PO_4 levels in groundwater (> 1 mg/L), suggesting lower P removal compared to N during treatment. The high irrigation volumes likely facilitate PO_4 breakthrough, reducing its retention in the subsurface. These findings have implications for nutrient stoichiometries in areas where this wastewater is reused or discharged, potentially affecting marine ecosystems via submarine groundwater discharge or

direct discharge. This requires further investigation.

This study improves the understanding of groundwater quality on Curaçao, demonstrating how inadequate sewage management through leaking cesspits and treated wastewater reuse leads to widespread nutrient contamination, while also providing significant anthropogenic freshwater recharge. Although the inclusion of private wells in urban areas may bias sampling toward more contaminated locations, these wells reflect the water quality to which people are directly exposed. This underscores the need for a more representative groundwater monitoring network that accounts for spatial, depth, and land use variability. Additionally, improving wastewater management and groundwater monitoring will improve water management on Curaçao and similar Caribbean islands, and help protect groundwater-affected ecosystems, such as nearshore coral reefs. The applied methodology using hydrochemical indicators (e.g. nutrient concentrations, nitrate isotopes, and Cl/B ratios) provides a useful framework for assessing groundwater contamination in other Small Island Developing States (SIDS) facing similar challenges.

CRediT authorship contribution statement

Boris M. van Breukelen: Writing – review & editing, Supervision, Project administration, Methodology, Funding acquisition, Conceptualization. **Victor F. Bense:** Writing – review & editing, Supervision, Funding acquisition, Conceptualization. **Titus P. Kruijssen:** Writing – review & editing, Investigation, Data curation. **Jessie-Lynn van Egmond:** Investigation, Data curation. **Mike R. J. Wit:** Writing – review & editing, Writing – original draft, Visualization, Validation, Methodology, Investigation, Formal analysis, Data curation, Conceptualization.

Declaration of generative AI and AI-assisted technologies in the writing process

During the preparation of this article the author(s) used ChatGPT (OpenAI, version 4o) in order to improve readability and streamline the text by removing redundancies. After using this tool, the author(s) manually reviewed and edited the content to ensure accuracy and take(s) full responsibility for the content of the final manuscript.

Declaration of Competing Interest

The authors declare that they have no known competing financial interests or personal relationships that could have appeared to influence the work reported in this paper.

Acknowledgements

This publication is part of the SEALINK project within the NWO Caribbean research programme (project number 5160958250), funded by the Dutch Research Council (NWO). We extend our gratitude to the people of Curaçao who helped us find suitable locations and allowed us to measure their wells. We also thank the Curaçao Ministry of Health, Environment, and Nature (GMN) and department of Agriculture, Livestock, and Fisheries (LVV) for providing valuable historical data and granting access to their sites. Special appreciation goes to Gerard van Buurt for his invaluable knowledge and insights on Curaçao's history and environment. We are grateful to Carmabi for use of their lab and general assistance during fieldwork on Curaçao, especially Mark Vermeij (UvA, Carmabi). We thank Jasper de Goei (UvA) for DOC analysis, Andrew Smith (British Geological Survey) for nitrate isotope analysis, and Patricia van den Bos, Armand Middeldorp, and Jane Erkemeij (TU Delft Waterlab) for chemical analysis. We like to thank Iris Verstappen for assisting in the field and conducting lab work. Additionally, we appreciate the valuable feedback provided by Nadia van Pelt (Centre for Languages and Academic Skills, ITAV). We thank the reviewers and editors for their valuable feedback, which greatly improved the clarity of the manuscript.

Appendix A. Supporting information

Supplementary data associated with this article can be found in the online version at doi:10.1016/j.ejrh.2025.102555.

Data availability

Data will be made available on request.

References

Abtmaier, B.F., 1978. Groundwater investigation Curaçao. Isl. Gov. Curaçao 290.

Adegoke, A., and T. Stenstrom, 2019, Cesspits and soakpits, in J. B. Rose, and B. Jiménez-Cisneros, eds., Global Water Pathogen Project Part 4 Management of Risk from Extreta and Wastewater, UNESCO.

UOOW, pers. comm., Effluentverbruik Oost en West 2017-2019, Uitvoeringsorganisatie Openbare Werken, Unpublished

Ahmed, F., Mishra, V., 2020. Estimating relative immediacy of water-related challenges in Small Island Developing States (SIDS) of the Pacific Ocean using AHP modeling. Model. Earth Syst. Environ. v. 6, 201–214.

Alcalá, F.J., Custodio, E., 2008. Using the Cl/Br ratio as a tracer to identify the origin of salinity in aquifers in Spain and Portugal. J. Hydrol. v. 359, 189–207.

Altabet, M.A., Wassenaar, L.I., Douence, C., Roy, R., 2019. A Ti(III) Reduct. Method Onestep Convers. Seawater Freshw. Nitrate into N. (2) O stable Isot. Anal. (15) N. /(14) N. (18) O/(16) O (17) O/(16) O Rapid Commun. Mass Spectrom. v. 33, 1227–1239.

Appelo, C.A.J., Postma, D., 2005. Groundw. Pollut. 647.

Aqualectra, 2021. Annual Report 2021. Aqualectra.

Barth, S., 1998. Application of boron isotopes for tracing sources of anthropogenic contamination in groundwater. Water Res. v. 32, 685–690.

Beckman, G.G., Thompson, C.H., Hubble, G.D., 1974. Genesis of red and black soils on basalt on the Darling Downs, Queensland, Australia: European. J. Soil Sci. v. 25, 265–281.

Beets, D.J., 1972, Lithology and stratigraphy of the Cretaceous and Danian succession of Curaçao, *in* {C}{C}U. o. {C}{C}Utrecht{C}{C}, ed{C}{C}.

Beets, D.J., 1977. Guide to the field excursions on Curaçao, Bonaire and Aruba, Netherlands Antilles - Cretaceous and Early Tertiary of Curacao, 8th Caribbean Geological Conference. GUA Pap. Geol. 7–17.

Bejannin, S., Tamborski, J.J., van Beek, P., Souhaut, M., Stieglitz, T., Radakovitch, O., Claude, C., Conan, P., Pujo-Pay, M., Crispi, O., Le Roy, E., Estournel, C., 2020. Nutrient Fluxes Associated With Submarine Groundwater Discharge From Karstic Coastal Aquifers (Côte Bleue, French Mediterranean Coastline). Front. Environ. Sci. v. 7.

Bellomo, S., N. Luengo-Oroz, and W. D'Alessandro, 2014, High Vanadium concentrations in groundwater at El Hierro (Canary Islands, Spain), 10th International Hydrogeological Congress of Greece / Thessaloniki, Thessaloniki, Greece.

Blach, O., 2015. Making rain: can technology drought-proof the Caribbean? Guardian.

Bonnélye, V., Sanz, M.A., Francisci, L., Beltran, F., Cremer, G., Colcuera, R., Laraudogoitia, J., 2007. Curacao, Netherlands Antilles: A successful example of boron removal on a seawater desalination plant. Desalination v. 205, 200–205.

Böttcher, J., Strebel, O., Voerkelius, S., Schmidt, H.L., 1990. Using isotope fractionation of nitrate-nitrogen and nitrate-oxygen for evaluation of microbial denitrification in a sandy aquifer. J. Hydrol. v. 114, 413–424.

Bruggenwert, M.G.M., Kamphorst, A., 1979. Survey of Experimental Information on Cation Exchange in Soil Systems, *in* G. H. Bolt, ed. Developments in Soil Science. In: Soil Chemistry: B. Physico-Chemical Models, v. 5. Elsevier Scientific Publishing Company, pp. 141–203.

Cannonier, C., Burke, M.G., 2019. The economic growth impact of tourism in Small Island Developing States - evidence from the Caribbean. Tour. Econ. v. 25, 85–108.

CaribDA, Caribbean Desalination Association.

CBSC, 2011, Census Curaçao 2011, *in* C. B. o. S. Curaçao, ed., Willemstad.

CBSC, 2021. Curaçao Environmental Statistics Compendium 2020. Willemst. Cent. Bur. Stat. Curaçao 76.

CBSC, 2024a, Eerste resultaten Census 2023, in C. B. o. S. Curaçao, ed., p. 26.

CBSC, 2024b, Tourism, Central Bureau of Statistics Curaçao.

Cey, E.E., Rudolph, D.L., Aravena, R., Parkin, G., 1999. Role of the riparian zone in controlling the distribution and fate of agricultural nitrogen near a small stream in southern Ontario. J. Contam. Hydrol. v. 37, 45–67.

CIWC, 2020, De toekomst van Water - Beleidsplan voor integraal waterbeheer, in {C}C.I.W. Curacao, ed{C}.

Cloutier, V., Lefebvre, R., Therrien, R., Savard, M.M., 2008. Multivariate statistical analysis of geochemical data as indicative of the hydrogeochemical evolution of groundwater in a sedimentary rock aquifer system. J. Hydrol. v. 353, 294–313.

Crabit, A., Cattan, P., Colin, F., Voltz, M., 2016. Soil and river contamination patterns of chlordecone in a tropical volcanic catchment in the French West Indies (Guadeloupe). Environ. Pollut. v. 212, 615–626.

D'Angelo, C., Widenmann, J., 2014. Impacts of nutrient enrichment on coral reefs: new perspectives and implications for coastal management and reef survival. Curr. Opin. Environ. Sustain. v. 7, 82–93.

Davis, S.N., Whittemore, D.O., Fabryka-Martin, J., 1998. Uses of Chloride/Bromide Ratios in Studies of Potable Water. Groundwater v. 36, 338–350.

de Vries, A.J., 2000. The semi-arid environment of Curaçao: a geochemical soil survey. Neth. J. Geosci. Geol. En. Mijnb. v. 79, 479–494.

Debrot, D., 2015. Slim samenwerken met de natuur. Herbebossing op de Nederlands-Caribische Benedenwindse Eilanden. Vakblad Natuur Bos Landschap.

Dillon, P., 1999, Groundwater pollution by sanitation on tropical islands, Paris, International Hydrological Programme, p. 34.

Dotsika, E., Poutoukis, D., Kloppmann, W., Guerrot, C., Voutsa, D., Kouimtzis, T.H., 2010. The use of O, H, B, Sr and S isotopes for tracing the origin of dissolved boron in groundwater in Central Macedonia, Greece. Appl. Geochem. v. 25, 1783–1796.

DOW, 1991, Afvalwaterstructuurplan Curaçao, *in* {C}{C}D.O. Werken, ed{C}{C}., p. 46.

Dupont, M.F., Elbourne, A., Cozzolino, D., Chapman, J., Truong, V.K., Crawford, R.J., Latham, K., 2020. Chemometrics for environmental monitoring: a review. Anal. Methods v. 12, 4597–4620.

Edwards, Q.A., Sultana, T., Kulikov, S.M., Garner-O'Neale, L.D., Metcalfe, C.D., 2019. Micropollutants related to human activity in groundwater resources in Barbados, West Indies. Sci. Total Environ. v. 671, 76–82.

Eiswirth, M., Hötzl, H., 1997. Impact Leak. Sewers Urban Groundw. Groundw. Urban Environ. 399–404.

Falkenmark, M., Chapman, T., 1989. Comparative hydrology: an ecological approach to land and water resources. UNESCO, p. 479.

Falkland, A., 1991. Hydrology and water resources of small islands: a pratical guide. UNESCO, Paris, France.

Falkland, T., 1999. Water resources issues of small island developing states. Nat. Resour. Forum v. 23, 245–260.

FAO, 1994, Water quality for agriculture, in F. a. A. O. o. t. {C}{C}U. Nations, ed{C}{C}., Rome.

Fidelibus, M.D., I. Morell, E.G. Giménez-Forcada, and L. Tulipano, 1993, Salinization processes in the Castellon Plain Aquifer (Spain), Proceedings 12th Saltwater Intrusion Meeting, Barcelona, p. 267-283.

Fouke, B.W., Beets, D.J., Meyers, W.J., Hanson, G.N., Mielillo, A.J., 1996. 87Sr/86Sr Chronostratigraphy and Dolomitization History of the Seroe Domi Formation, Curaçao (Netherlands Antilles). Facies v. 35, 293–320.

Fukada, T., Hiscock, K.M., Dennis, P.F., Grischek, T., 2003. A dual isotope approach to identify denitrification in groundwater at a river-bank infiltration site. Water Res. v. 37, 3070–3078.

Fustec, E., Mariotti, A., Grillo, X., Sajus, J., 1991. Nitrate removal by denitrification in alluvial groundwater: role of a former channel. J. Hydrol. v. 123, 337–354.

Gillham, R.W., Cherry, J.A., 1978. Field evidence of denitrification in shallow groundwater flow systems. Water Pollut. Res. Cana v. 13, 53–72.

Gohar, A.A., Cashman, A., Ward, F.A., 2019. Managing food and water security in Small Island States: New evidence from economic modelling of climate stressed groundwater resources. J. Hydrol. v. 569, 239–251.

Gordon-Smith, D.-A.D.S., Greenaway, A.M., 2019. Submarine groundwater discharge and associated nutrient fluxes to Discovery Bay, Jamaica. Estuar. Coast. Shelf Sci. v. 230.

Gourcy, L., Baran, N., Vittecoq, B., 2009. Improving the knowledge of pesticide and nitrate transfer processes using age-dating tools (CFC, SF6, 3H) in a volcanic island (Martinique, French West Indies). J. Contam. Hydrol. v. 108, 107–117.
Govers, L.L., Lamers, L.P., Bouma, T.J., De Brouwer, J.H.F., van Katwijk, M.M., 2014. Eutrophication threatens Caribbean seagrasses - An example from Curaçao and Bonaire. Mar. Pollut. Bull. v. 89, 481–486.
Granger, J., Wankel, S.D., 2016. Isotopic overprinting of nitrification on denitrification as a ubiquitous and unifying feature of environmental nitrogen cycling. Proc. Natl. Acad. Sci. v. 113, 6391–6400.
Griffioen, J., 2001. Potassium adsorption ratios as an indicator for the fate of agricultural potassium in groundwater. J. Hydrol. v. 254, 244–254.
Grontmij and Sogreah, 1968. Water and land resources development plan for the island of Aruba, Bonaire and Curaçao.
Güler, C., Kurt, M.A., Alpaslan, M., Akbulut, C., 2012. Assessment of the impact of anthropogenic activities on the groundwater hydrology and chemistry in Tarsus coastal plain (Mersin, SE Turkey) using fuzzy clustering, multivariate statistics and GIS techniques. J. Hydrol. v. 414-415, 435–451.
Harris, S.J., Cendón, D.I., Hankin, S.I., Peterson, M.A., SXiao, S., Kelly, B.F.J., 2022. Isotopic evidence for nitrate sources and controls on denitrification in groundwater beneath an irrigated agricultural district. Sci. Total Environ. v. 817.
Henriquez, P.C., 1962, Problems relating to hydrology, water conservation, erosion control, reforestation and agriculture in Curaçao: Natuurwetenschappelijke werkgroep Nederlandse Antillen, v. 14, p. 1-54.
Herweijer, J.P., Buisonjé, P.H. d, Zonneveld, J.I.S., 1977. Guide to the field excursions on Curaçao, Bonaire and Aruba, Netherlands Antilles - Neogene and Quaternary geology and geomorphology. 8th Caribb. Geol. Conf. GUA Pap. Geol. 39–55.
Holding, S., Allen, D.M., Foster, S., Hsieh, A., Larocque, I., Klassen, J., Van Pelt, S.C., 2016. Groundwater vulnerability on small islands. Nat. Clim. Change v. 6, 1100–1103.
Houk, P., Castro, F., McInnis, A., Rucinski, M., Starsinic, C., Concepcion, T., Manglona, S., Salas, E., 2022. Nutrient thresholds to protect water quality, coral reefs, and nearshore fisheries. Mar. Pollut. Bull. v. 184.
Jones, R., Parsons, R., Watkinson, E., Kendell, D., 2011. Sewage contamination of a densely populated coral 'atoll' (Bermuda). Environ. Monit. Assess. v. 179, 309–324.
Kaehler, C.A., and B. Kenneth, 2003, Tracing reclaimed water in the Menifee, Winchester, and Perris south groundwater subbasins, Riverside County, California, U.S. Geological Survey.
Kendall, C., 1998. Tracing nitrogen sources and cycling in catchments *in* C. Kendall, and J. J. McDonnell, eds. Isotope Tracers in Catchment Hydrology: Amsterdam. Elsevier Science B.V, pp. 519–576.
Kendall, C., Caldwell, E.A., 1998. Fundamentals of Isotope Geochemistry, *in* C. Kendall., and J. J. McDonnell, eds. Isotope Tracers in Catchment Hydrology Amsterdam. Elsevier Science B.V, pp. 51–86.
Kerr, A.C., Tarney, J., Marriner, G.F., Klaver, G.T., Saunders, A.D., Thirlwall, M.F., 1996. The geochemistry and petrogenesis of the late-Cretaceous picrites and basalts of Curaçao, Netherlands Antilles: a remnant of an oceanic plateau. Contrib. Mineral. Petrol. v. 124, 29–43.
Kim-Hak, D., Dixon, M.B., Galan, M.A., Boisseau, F., Gallastegui, J., Martina, R., 2014. Santa Barbara, Curacao desalination plant expansion using NanoH2O thin film nanocomposite (TFN) SWRO membrane. Desalin. Water Treat. v. 55, 2446–2452.
Klaver, G.T., 1987. The Curaçao Lava Formation: an ophiolitic analogue of the anomalous thick layer 2B of the mid-Cretaceous oceanic plateaus in the western Pacific and. Cent. Caribb. GUA Pap. Geol.
Kloppmann, W., Van Houtte, E., Picot, G., Vandenbohede, A., Lebbe, L., Guerrot, C., Millot, R., Gaus, I., Wintgens, T., 2008a. Monitoring reverse osmosis treated wastewater recharge into a coastal aquifer by environmental isotopes (B, Li, O, H). Environ. Sci. Technol. v. 42, 8759–8765.
Kloppmann, W., Vengosh, A., Guerrot, C., Millot, R., Pankratov, I., 2008b. Isotope and Ion selectivity in Reverse Osmosis desalination: geochemical tracers for man-made freshwater. Environ. Sci. Technol. v. 42, 4723–4731.
Koba, K., Tokuchi, N., Wada, E., Nakajima, T., Iwatsubo, G., 1997. Intermittent denitrification: The application of a 15N natural abundance method to a forested ecosystem. Geochim. Et. Cosmochim. Acta v. 61, 5043–5050.
Kroopnick, P., Craig, H., 1972. Atmospheric oxygen: isotopic composition and solubility fractionation. Science v. 175, 54–55.
Kruijssen, T., Wit, M., Van Breukelen, B.M., Van der Ploeg, M., Bense, V.F., 2024. Hydrogeological conceptualization of a small island groundwater system using historical data. Neth. J. Geosci. v. 103.
Louws, R.J., Vriend, S.P., Frapporti, G., 1997. De grondwaterkwaliteit van Curaçao. Een Hydrogeochem. onderzoek. H2O 26 (v. nr).
Mandal, A., Haiduk, A., 2010. Hydrochemical characteristics of groundwater in the Kingston Basin, Kingston, Jamaica. Environ. Earth Sci. v. 63, 415–424.
Martinez-Santos, P., Martin-Loeches, M., Garcia-Castro, N., Solera, D., Diaz-Alcaide, S., Montero, E., Garcia-Rincon, J., 2017. A survey of domestic wells and pit latrines in rural settlements of Mali: Implications of on-site sanitation on the quality of water supplies. Int J. Hyg. Environ. Health v. 220, 1179–1189.
Mayer, B., Bollwerk, S.M., Mansfeldt, T., Hütter, B., Veizer, J., 2001. The oxygen isotope composition of nitrate generated by nitrificaion in acid forest floors. Geochim. Et. Cosmochim. Acta v. 65, 2743–2756.
McArthur, J.M., Sikdar, P.K., Hoque, M.A., Ghosal, U., 2012. Waste-water impacts on groundwater: Cl/Br ratios and implications for arsenic pollution of groundwater in the Bengal Basin and Red River Basin, Vietnam. Sci. Total Environ. v. 437, 390–402.
MDC, 2024, Meteorological Department of Curaçao.
Molengraaff, G.J.H., 1929, Geologie en geohydrologie van het eiland Curaçao, *in* {C}T.H. Delft, ed{C}., Delft, T.H.S. Biobliotheek Delft, p. 196.
Monjerezi, M., Vogt, R.D., Gebru, A.G., Saka, J.D.K., Aagaard, P., 2012. Minor element geochemistry of groundwater from an area with prevailing saline groundwater in Chikhwawa, lower Shire valley (Malawi). Phys. Chem. Earth Parts A/B/C. v. 50-52, 52–63.
Muir, K.S., and T.B. Coplen, 1981, Tracing groundwater movement by using the stable isotopes of oxygen and hydrogen, Upper Penitencia Creek Alluvial Fan, Santa Clara Valley, California: Geological Survey Water-supply paper.
Ostrom, N.E., Hedin, L.O., von Fischer, J.C., Robertson, G.P., 2002. Nitrogen Transformations and NO 3 - Removal at a Soil-Stream Interface: A Stable Isotope Approach. Ecol. Appl. v. 12.
Otero, N., Torrentó, C., Soler, A., Menció, A., Mas-Pla, J., 2009. Monit. Groundw. Nitrate attenuation a Reg. Syst. coupling Hydrogeol. multiIsot. Methods. case Plana De. Vic. (Osona Spain) Agric. Ecosyst. Environ. v. 133, 103–113.
Parkhurst, D.L., Appelo, C.A.J., 2013. Description of input and examples for PHREEQC version 3 - A computer program for speciation, batch-reaction, one-dimensional transport, and inverse geochemical calculations. U. S. Geol. Surv. 497.
Podgorski, J., Berg, M., 2022. Global analysis and prediction of fluoride in groundwater. Nat. Commun. v. 13.
Rawlins, B.G., Ferguson, A.J., Chilton, P.J., Arthurtons, R.S., Grees, J.G., 1998. Review of agricultural pollution in the Caribbean with particular emphasis on small island developing states. Mar. Pollut. Bull. v. 36, 658–668.
Russo, R., Sciacca, S., La Milia, D.I., Poscia, A., Moscato, U., 2014. Vanadium in drinking water: toxic or therapeutic?! Systematic literature review and analysis of the population exposure in an Italian volcanic region: Roberta Russo. Eur. J. Public Health v. 24.
Santos, I.R., Chen, X., Lecher, A.L., Sawyer, A.H., Moosdorf, N., Rodellas, V., Tamborski, J., Cho, H.-M., Dimova, N., Sugimoto, R., Bonaglia, S., Li, H., Hajati, M.-C., Li, L., 2021. Submarine groundwater discharge impacts on coastal nutrient biogeochemistry. Nat. Rev. Earth Environ. v. 2, 307–323.
Sawhney, B.L., 1972. Selective Sorption and Fixation of Cations by Clay Minerals: A Review. Clays Clay Miner. v. 20, 93–100.
Scanlon, B.R., Keese, K.E., Flint, A.L., Flint, L.E., Gaye, C.B., Edmunds, W.M., Simmers, I., 2006. Global synthesis of groundwater recharge in semiarid and arid regions. Hydrol. Process. v. 20, 3335–3370.
Steward, R., Chopin, P., Verburg, P.H., 2025. Impact-driven spatial planning for future-proofing small island states: A scenario-based land model analysis in Curaçao. Appl. Geogr. v. 178.
STINAPA, 1977, Guide to the field excursions on Curacao, Bonaire and Aruba, Netherlands Antilles: GUA Papers of Geology, 120 p.
Strande, L., Evans, B., von Sperling, M., Bartram, J., Harada, H., Nakagiri, A., Nguyen, V.A., 2023. Urban Sanitation: New Terminology for Globally Relevant Solutions? Environ. Sci. Technol. v. 57, 15771–15779.
Stueber, A.M., Criss, R.E., 2005. Origin and transport of dissolved chemicals in a karst watershed, southwestern Illinois. J. Am. Water Resour. Assoc. v. 41, 267–290.

Teixeira, P.C., Ordens, C.M., McIntyre, N., Pagliero, L., Crosbie, R., 2023. Spatio-temporal distribution of atmospheric chloride deposition over a small island. Hydrol. Process. v. 37.
TNO-GDN, 2021, Geologische kaart van het Koninkrijk der Nederlanden 1: 600 000, in T.G.D. Nederland, ed., Utrecht, Utrecht isbn: 97890-5986-514-3., p. 1.
Torres-Martinez, J.A., Mora, A., Knappett, P.S.K., Ornelas-Soto, N., Mahlknecht, J., 2020. Tracking nitrate and sulfate sources in groundwater of an urbanized valley using a multi-tracer approach combined with a Bayesian isotope mixing model. Water Res v. 182, 115962.
Tweed, S.O., Weaver, T.R., Cartwright, I., 2005. Distinguishing groundwater flow paths in different fractured-rock aquifers using groundwater chemistry: Dandenong Ranges, southeast Australia. Hydrogeol. J. v. 13, 771–786.
UNOPS, 2018. Evidence-based infrastructure: Curaçao. National infrastructure systems modelling to support sustainable and resilient infrastructure development, United Nations Office for Project Services (UNOPS),Infrastructure Transitions Research Consortium (ITRC),Ministry of Trafic, Transport and Urban Planning, p. 60.
Van der Molen, M., Buth, L., 1993. Afvalwaterbehandeling Curaçao gericht op hygiëne. Behoud.. Kwal. Oppervlaktew. En. Hergebruik Effl. H2O V. 26.
Van Meeteren, N., 1945. Watervoorziening en Grondwaterpeil op Curaçao. Lux. Jaar 3.
van Sambeek, M.H.G., Eggenkamp, H.G.M., Vissers, M.J.M., 2000. The groundwater quality of Aruba, Bonaire and Curaçao: a hydrogeochemical study. Neth. J. Geosci. Geol. En. Mijnb. v. 79, 459–466.
Vázquez-Suñé, E., Carrera, J., Tubau, I., Sánchez-Vila, X., Soler, A., 2010. An approach to identify urban groundwater recharge. Hydrol. Earth Syst. Sci. v. 14, 2085–2097.
VEI, 2013. Rapport detailonderzoek non-revenue water Curaçao. Vitens Evides International.
Waggott, A., 1969. An investigation of the potential problem of increasing boron concentrations in rivers and water courses. Water Res. v. 3.
Wilhelm, S.R., S.L. Schiff, and J.A. Cherry, 1994, Biochemical evolution of domestic wastewater in domestic septic systems, Section 1 - Conceptual model: Groundwater, v. 32.
Xu, S., Kang, P., Sun, Y., 2016. A stable isotope approach and its application for identifying nitrate source and transformation process in water. Environ. Sci. Pollut. Res Int v. 23, 1133–1148.
Xue, D., Botte, J., De Baets, B., Accoe, F., Nestler, A., Taylor, P., Van Cleemput, O., Berglund, M., Boeckx, P., 2009. Present limitations and future prospects of stable isotope methods for nitrate source identification in surface- and groundwater. Water Res v. 43, 1159–1170.
Zaneveld, J.R., Burkepile, D.E., Shantz, A.A., Pritchard, C.E., McMinds, R., Payet, J.P., Welsh, R., Correa, A.M., Lemoine, N.P., Rosales, S., Fuchs, C., Maynard, J.A., Thurber, R.V., 2016. Overfishing and nutrient pollution interact with temperature to disrupt coral reefs down to microbial scales. Nat. Commun. v. 7, 11833.